pH dependent conformational changes of the catalytic domain of deubiquitinase OTU1 from *Saccharomyces cerevisiae*

by

Herby Cadet

A Thesis submitted to the Faculty of Graduate Studies of
University of Manitoba
in partial fulfilment of the requirements for the degree of

Master of Science

Department of Chemistry
University of Manitoba
Winnipeg, Manitoba

Copyright © 2020, Herby Cadet

Abstract

Proteins often consist of linked domains which are regions of a protein sequence that can fold independently of each other. Domain dynamics are known to play an important role in enabling the formation of large proteins but there has not been much research done into how domains may affect protein folding and enzymatic activity. To gain insight into domain dynamics we will study the catalytic domain ScOTU1 of a model multi-domain deubiquitinase from yeast called OTU1 which catalyzes the breakdown of ubiquitin iso-peptide linkages. ScOTU1 was successfully overexpressed in BL21-DE3 cells and purified using a nickel column where it then underwent a rapid buffer exchange using a gel filtration column. ScOTU1 was studied utilizing two experiments a Ubiquitin-Rhodamine catalytic cleavage assay and a Bis-ANS hydrophobicity assay. Through cleavage of Ubiquitin-Rhodamine it was possible to measure the k_{cat}/Km specificity constant which showed significant activity at pH ranges from eight to seven. The Bis-ANS experiments showed that the ScOTU1 catalytic domain existed in two conformations that were shifted in a pH dependent manner. At high pH the ScOTU1 catalytic domain was present in a primarily open conformation and at low pH the ScOTU1 catalytic domain was present in a primarily closed conformation. The Ubiquitin-Rhodamine and Bis-ANS experiments provided evidence that the current model for catalytic cleavage of the iso-peptide linkages of a polyubiquitin molecule by ScOTU1 follows a conformation selection mechanism for enzyme catalysis which is a two-state mechanism where ScOTU1 is in an equilibrium between a closed and open conformation where at physiological pH the enzyme is primarily in a closed conformation. Through the binding of its polyubiquitin substrate the equilibrium can shift to enable catalysis to occur at physiological pH.

Acknowledgments

I would like to thank all those that aided me in completing this academic journey. The guidance of my supervisors Mazdak Khajehpour and Joe O'Neil, the patience of senior graduate students Mary Hernando and Ben Bailey-Elkin, and the support and encouragement from my family members and friends.

List of Tables

List of Figures

Chapter 1

Table of Contents

Chapter 1

Introduction

1.1 Protein Dynamics

For a protein to function, conformational dynamics are required that promote the adoption of the essential folded structures. These structures allow proteins to function in many roles including structural functions that maintain cell shape and additionally make up structural elements in connective tissue and a multitude of enzymatic functions[1]. The conformational motions required for these changes exist in a conformational energy landscape where there are peaks of high energy conformations and valleys of more stable low energy conformations[2]**.** It is interesting though, that proteins only sample a proportion of the conformational configurations available to them, a proportion that is hundreds of orders of magnitude smaller than what the full conformational space would allow[3]**.** A thought experiment coined Levinthal's Paradox states that a 60 amino acid protein, if left to sample all possible configurations, could take longer than the current age of the universe before it arrived at the correct conformation, a scenario that clearly cannot exist as we know the majority of proteins fold within a micro – millisecond timescale. Levinthal concluded that there must be some energy bias that reduced the conformational space that a protein samples[3,4].

The multitude of conformations and the reversible transformation from one to another coined, protein dynamics, is often lost or disturbed in most structural analyses of proteins *via* techniques such as x-ray crystallography or mass spectroscopy and in the case of NMR there is a size limitation to the proteins that can be studied[5,6]. Techniques involving molecular dynamics simulations have also been developed to probe the conformational landscape and have proven to be successful but computational power remains the limiting factor when studying the dynamics of larger proteins[7]

Finding novel methods to explore the dynamic states of proteins would not only provide us with knowledge for future projects such as artificial protein design for pharmaceutical uses but would allow insight into the evolution of proteins. Dynamics studies could for example explain why the foldable length limit of a protein is approximately 200 amino acids with current studies indicating the cause to be a general protein folding force called the hydrophobic effect[3].The foldable length limit is the theoretical maximum amino acid content of a protein which if exceeded results in a protein that would no longer fold within a biologically relevant time scale. This maximum is based upon the reduced effectiveness of the hydrophobic effect on protein folding as a protein's amino acid sequence increases[3]. The hydrophobic effect is a force which results in the global tendency for an amino acid chain to collapse into a compact shape in conjunction with the segregation of hydrophobic and hydrophilic residues to the interior and exterior of a protein respectively[8].

A 200 amino acid limit is certainly strange as there currently exists proteins that greatly exceed this limit such as the 2000 residue 5 MDa adhesin found in the Antarctic bacterium *Marinomonas primoryensis*[9]**.** To circumvent this 200 amino acid limit, proteins such as the adhesin have evolved to include multiple domains which are short regions within a protein sequence that can fold, function, and exist independently of the rest of the protein. Protein domains have also been shown to play vital roles in creating diversity in protein architectures and enabling protein evolution[10]. These domains are typically only 100-200 amino acids in length which falls within the region limited by the hydrophobic effect[3].

Different multidomain proteins have evolved through recombination and duplication of a limited set of stable and well folding domains. Through recombination these multidomain proteins have achieved new folds, functions and protein architectures[11]. The effect that individual protein domains have on one another with respect to folding and stability is not currently well understood

but in recent years studies have shown that there exist interdomain interactions that can stabilize the tertiary structures of proteins[12] some of which also aid directly with a protein's catalytic mechanism in the case of enzymes[13].

Interdomain interactions have been shown to affect a protein's activity and stability but with more research done it could allow for the design of more efficient medicines for various protein-based diseases and could help in producing new proteins while providing a greater understanding of the many proteins present in organisms including humans. To gain a deeper understanding of multidomain proteins and their interactions a yeast multi-domain protein called the Ovarian Tumor Domain protease "OTU1" from *Saccoromyces cerevisiae* was investigated in this work.

1.1.2 Protein Binding Models

Enzymes such as OUT1 when free in solution do not typically exist in an active state. They often require interaction with a specific substrate to adopt an active conformation. Many models such as the induced fit model, fly-casting model, and conformational selection model have been proposed as mechanisms by which to describe the interaction between substrate and enzyme**14**. The induced fit model suggests that binding events change the conformation of both the enzyme and substrate. These substrate-induced changes have been shown to bring catalytic residues into alignment, alter the local environment, and position the substrate for catalysis. The fly-casting model proposes that once a protein crosses a certain distance threshold a partially folded conformation of the enzyme can form some weak initial contacts which extends the enzymes binding radius**15**. The initial binding events then allow the protein to pull itself into the substrate which results in the completion of folding and binding as one conformational change where catalysis can then occur**16,17**. The conformational selection model in contrast to the induced fit model suggest that an enzyme samples many conformations prior to substrate binding. Once the enzyme has found a

conformation that compliments the structure of a substrate they can now bind where the substrate will further stabilize the selected conformation of the enzyme**18**. The mechanism by which OUT1 achieves an active conformation will be investigated in this work.

1.2 OTU1

The OTU1 enzyme in yeast is a multidomain protein that consists of 3 domains, where a protein domain is a highly conserved region of a protein sequence that can fold, function, and exist independently of the remainder of the protein chain[10]. The 3 domains of OTU1 consist of a ubiquitin like domain (UBX), a catalytic domain (ScOTU1), and a zinc binding domain (Zn)[19]. The 9.5 kDa UBX domain has been shown to aid in the formation and stabilization of the proteasome by forming positive interactions with valosin-containing protein (VCP) which is a AAA+ ATPase that aids in the recruitment of components to form the ERAD protein degradation complex[20]. The 4.3 kDa zinc binding domain is less well understood as it exists as an intrinsically disordered region of the protein[19] but it has been suggested that its zinc finger motif plays a role in the binding and recognition of ubiquitin. Zinc-finger motifs are commonly found in DNA binding and other proteins[21]. The 20 kDa catalytic ScOTU1 domain contains the catalytic triad of cysteine 120, which is within a disordered loop region of ScOTU1, and histidine 222 and aspartic acid 224 which are both in present in the same beta-sheet secondary structure element. The catalytic triad of residues function together to cleave the iso-peptide bonds[22] of ubiquitin chains in a mechanism shown in Figure 1. Through x-ray crystallography studies of ScOTU1, Messick et al. (2005) have found that there are three major hydrophobic contact regions between the ScOTU1 domain and ubiquitin molecules which may aid in the recognition of ubiquitin and/or in the stabilization of the catalytic domain to enable catalysis to occur at physiological pH[19] as described in Figure 2.

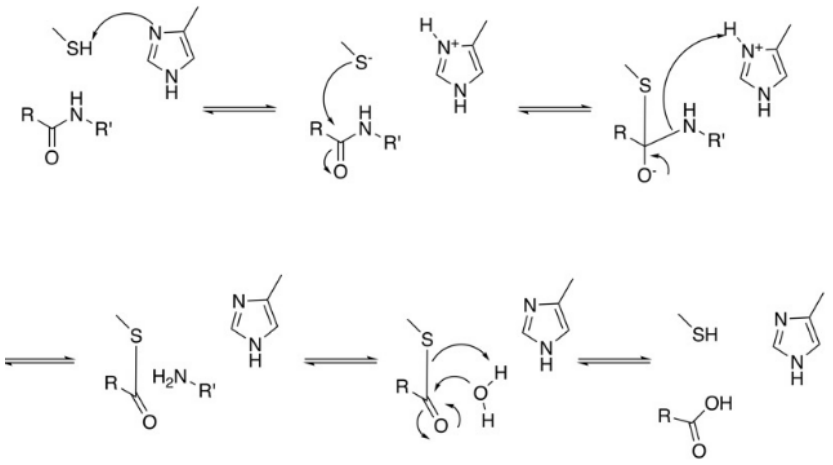

Figure 1. Mechanistic description of the cleavage of peptide bonds by the catalytic triad consisting of cysteine, histidine, and aspartic acid. Not shown is aspartic acid which increases the nucleophilicity of histidine to enable the extraction of a proton from cysteine[23].

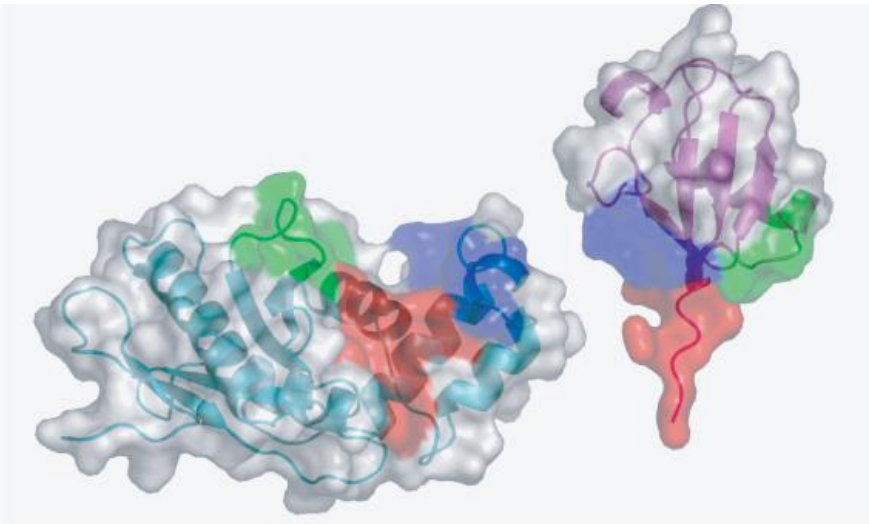

Figure 2. 3.4 Å x-ray crystallography structure showing the 3 main contact regions of solely ScOTU1 (left) to ubiquitin (right). The contact regions are represented by the colours blue green and red where the red region highlights the catalytic cleft and the area of greatest interaction between OTU1 and ubiquitin[19].

1.3 Ubiquitin

Ubiquitin is a highly conserved 76 kDa protein which acts as an important signalling molecule, a key component in many eukaryotic signal transduction pathways, a defining characteristic that has been pervasive in eukaryotes since the evolution of the last common ancestor[24]. It is considered a foundational protein required for the regulation and homeostasis of the eukaryotic proteome[25]. Ubiquitin's role in signalling pathways begins with ubiquitylation which is the formation of a bond between the c-terminal glycine amino acid of ubiquitin and the side chain amino group of a lysine residue of the target protein to form an initial iso-peptide bond[26]. Once ubiquitylated an E3 ubiquitin ligase can then add additional ubiquitins through the formation of iso-peptide bonds

through the linkage of the ubiquitin c-terminus and one of the seven ubiquitylated lysine side chain amino group residues present in a ubiquitin molecule[27].

Figure 3 is a diagram illustrating the multitude of biochemical pathways that involve ubiquitin which can range from DNA repair to proteasomal degradation, two vastly different processes. A ubiquitinated protein can be monoubiquitinated, multiubiquitinated, branched chain ubiquitinated, or polyubiquitinated with each altering the fate of the bound protein. Lysine 48 linked polyubiquitinated proteins are of great interest and will be discussed in more detail because they are the target of OTU1[28].

The proteasomal degradation pathways utilize lysine 48 to control the cell cycle through degradation of regulatory proteins *via* the proteasome[29]. This degradation motif is also a key component of the innate immune response of eukaryotes. It plays important regulatory roles in T cell, B cell, and Tumor Necrosis Factor signalling cascades all three of which are vital with regards to fighting off foreign viral and bacterial infections[30]. These signalling cascades must be tightly regulated by a sensitive and reversible mechanism which ubiquitylation provides, with the aim of avoiding excessive activation of the innate immune system which can result in chronic inflammation and various autoimmune disorders[31].

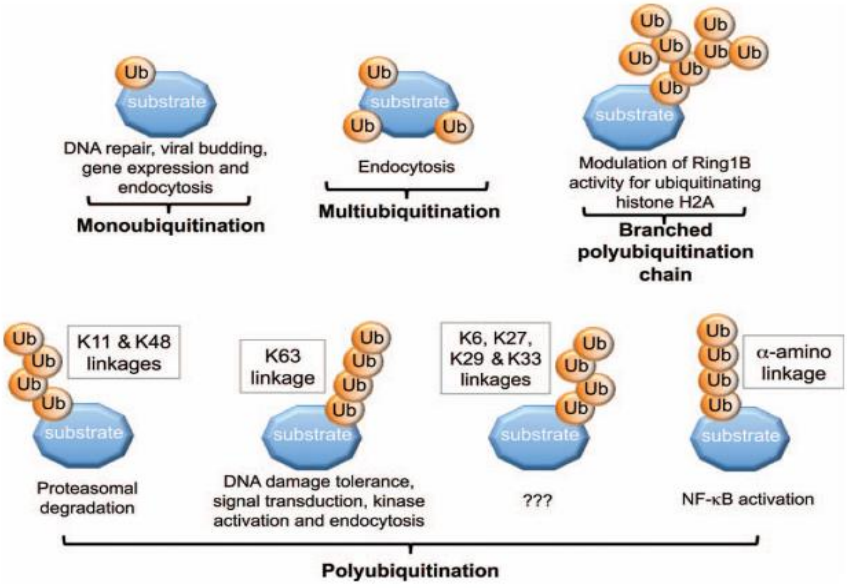

Figure 3. Illustration depicting the various methods by which a substrate may be bound by ubiquitin and how the different modes of ubiquitin binding lead to different substrate fates. Four major binding modes are exhibited which include monoubiquitination, multiubiquitination, branched polyubiquitination, and polyubiquitination. The differences in the fates of polyubiquitinated proteins lies with the type of lysine linkage that occurs as the ubiquitin chain is extended. Of particular interest is polyubiquitination through K11 or K48 which result in a proteasomal degradation pathway which OTU1 can alter and modify[27].

1.4 OTU1-Ubiquitin Interaction

OTU1 interacts preferentially with lysine 48-linked ubiquitin-bound proteins and therefore plays a role in both immune and proteolytic biochemical pathways[27, 30]. These pathways can be enhanced or disrupted by the presence or removal of OTU1 due to its ability to deconjugate the Lys-48 ubiquitin polymer or through the impairment of the endoplasmic reticulum associated-degradation pathway (ERAD)[19]. OTU1 is an important contributor to the ERAD pathway which is a protein quality control system that aims to destroy potentially toxic or misfolded membrane and secretory proteins which are synthesized in the endoplasmic reticulum[32]. OTU1 performs three important actions to enable the ERAD pathway to function. It forms electrostatic interactions with recruiter components of the proteasome which aid in the recruitment and stability of the proteasome[20]. As shown in Figure 4, OTU1 also interacts and forms stabilizing interactions with a cellular ATPase called CDC48 that separates polyubiquitinated targets from membranes or binding partners such as the removal of misfolded proteins from the endoplasmic reticulum for degradation in the proteasome[33]. The last important function of OTU1 is that once bound to CDC48 it can release the ubiquitin molecules bound to a protein tagged for destruction through iso-peptide bond cleavage. The proteins can then fully translocate through the ERAD complex where they can then be shuttled to the proteasome for recycling without unnecessary destruction of signalling ubiquitin molecules[33].

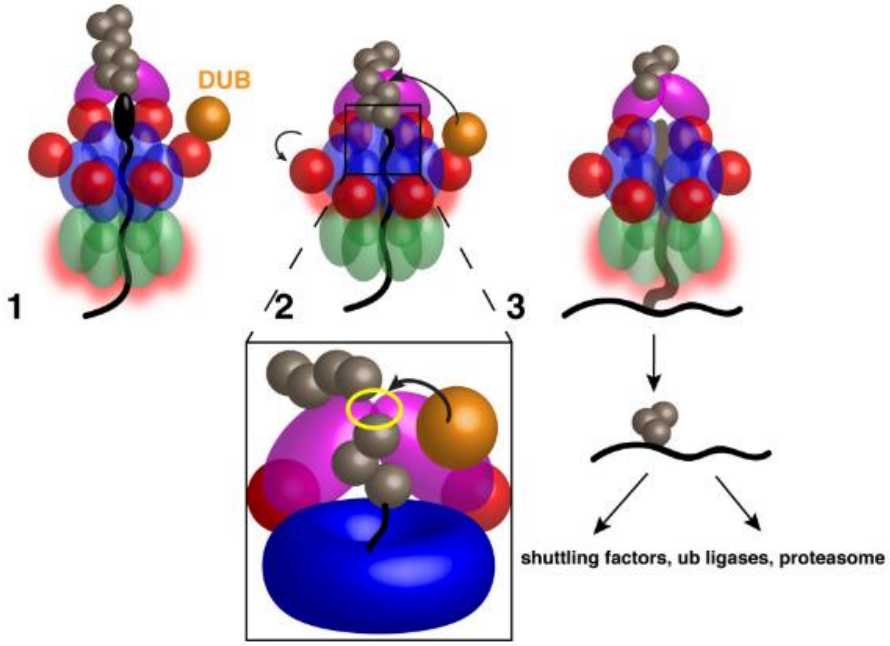

Figure 4. Mechanism of interaction between OTU1 with CDC48. Part 1: Protein (black) bound to ubiquitin (grey) travelling through CDC48 complex (red, blue, greed, purple). Part 2: Deubiquitinase- DUB (orange) cleaving ubiquitin linkages to allow for protein translocation through the CDC48 complex. Part 3: Protein released from CDC48 complex[33].

1.5 Viral and Bacterial OTU1 domains

Viruses and bacteria often encode deubiquitinases to cleave iso-peptide bonds of Lys-48 to negate any immune responses on the onset of infection by removal of ubiquitin moieties that signal foreign proteins for destruction through the proteasome[34,35]. *Chlamydia trachomatis* and *Chlamydia pneumoniae* are bacteria that contain an OTU-like domain. These two bacterial strains are known to play a role in acute and chronic genital and ocular infections[36], atherosclerosis, adult onset asthma, and Alzheimer's disease[37]. Many diseases such as cancers, autoimmune disorders, and inflammatory disorders can progress as the result of mutations in the genes that encode for OTU1 and other deubiquitinases.

1.6 The Dynamics of the OTU1 active site

Prior work on ScOTU1 by Roy Hutchings investigated the dynamics of the OTU1 active site by monitoring the binding of aldrithiol-4 a small molecule that binds irreversibly to thiol groups such as the lone cysteine residue that is present in the catalytic cleft of ScOTU1[38]. Experiments were performed at various pH values ranging from nine to seven as shown in Figure 5. The results suggest that at lower pH values there is less accessibility for Aldrithiol-4 to access the catalytic cysteine residue but as the pH is increased the probe can access the catalytic cysteine more readily. The results were analyzed using a kinetic model as shown in Figure 5.

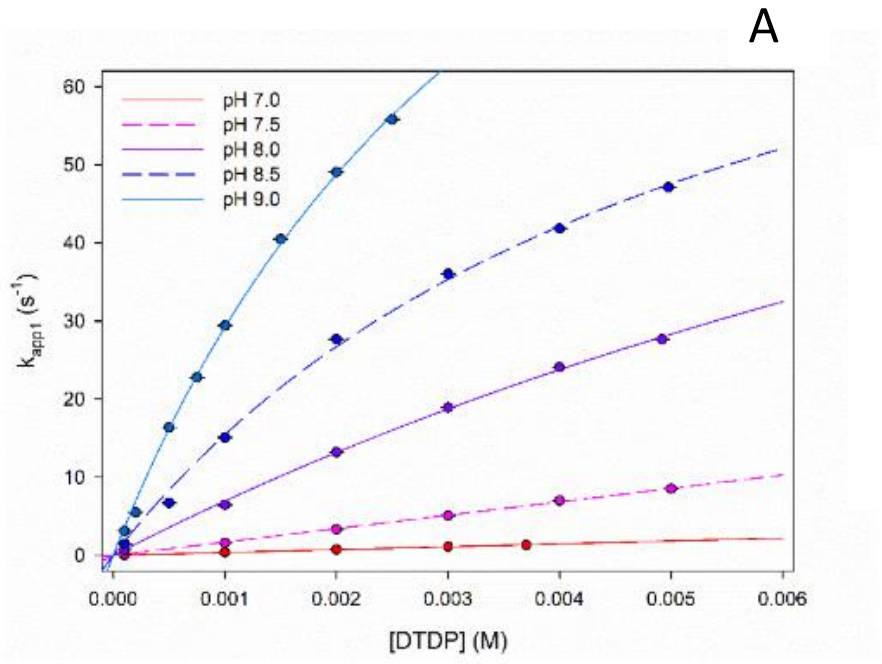

Figure 5. ***Otu1 pH dependent mechanism****. A, plot of the apparent rate constant of 2 µM ScOTU1 binding to aldrithiol-4 (DTDP) at various pH values. As pH is lowered a significant decrease in rate constant appears*[39]*. B, reaction kinetic scheme that shows a proposed mechanism whereby an equilibrium shift may occur for the free enzyme as exemplified by equilibrium constant* K_{E1} *which represents a closed conformation. As the pH of the solution is lowered the active site of the free enzyme may shift its equilibrium towards a more closed conformation decreasing accessibility to the DTDP to the catalytic cysteine residue.*

1.7 Fluorescence Spectroscopy

Fluorescence spectroscopy is a technique that is widely used for a variety of applications ranging across biotechnology, medical diagnostics, and genetic analysis. It is an inexpensive and highly sensitive technique that has the capability to provide a measure of the local and global changes in a protein's structure as well as dynamics information[40]. Figure 6(A) shows a schematic diagram outlining the configuration of a spectrofluorometer. Excitation typically begins with the use of a xenon lamp because they are capable of outputting high intensity light at all visible wavelengths above 250 nm. The excitation light then passes through an excitation monochromator and later an emission monochromator which both function to select a wavelength. The beam splitter is used to reflect shorter wavelengths onto the sample while transmitting longer wavelengths into a barrier filter and reflecting scattered excitation light back in the direction of the xenon lamphouse[41]. Figure 6(B) shows the instrument used to complete all fluorescence based experiments.

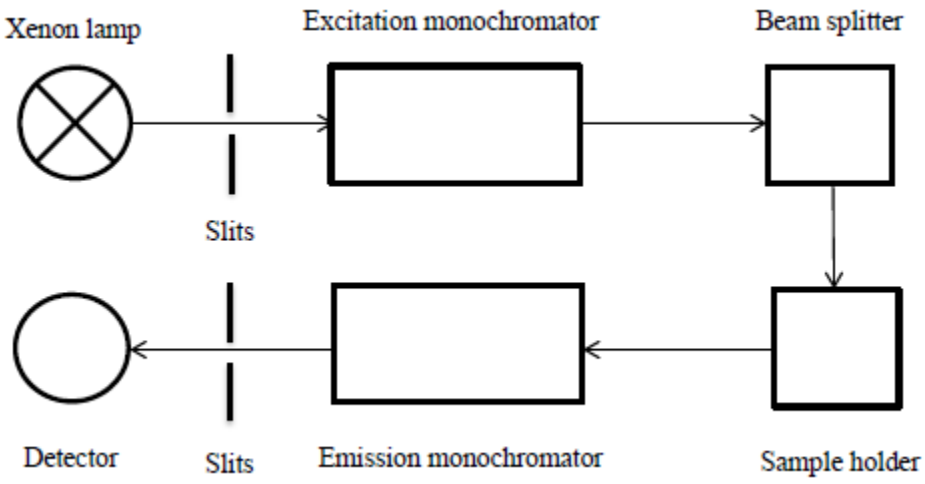

Figure 6. A, Schematic diagram of a spectrofluorometer.

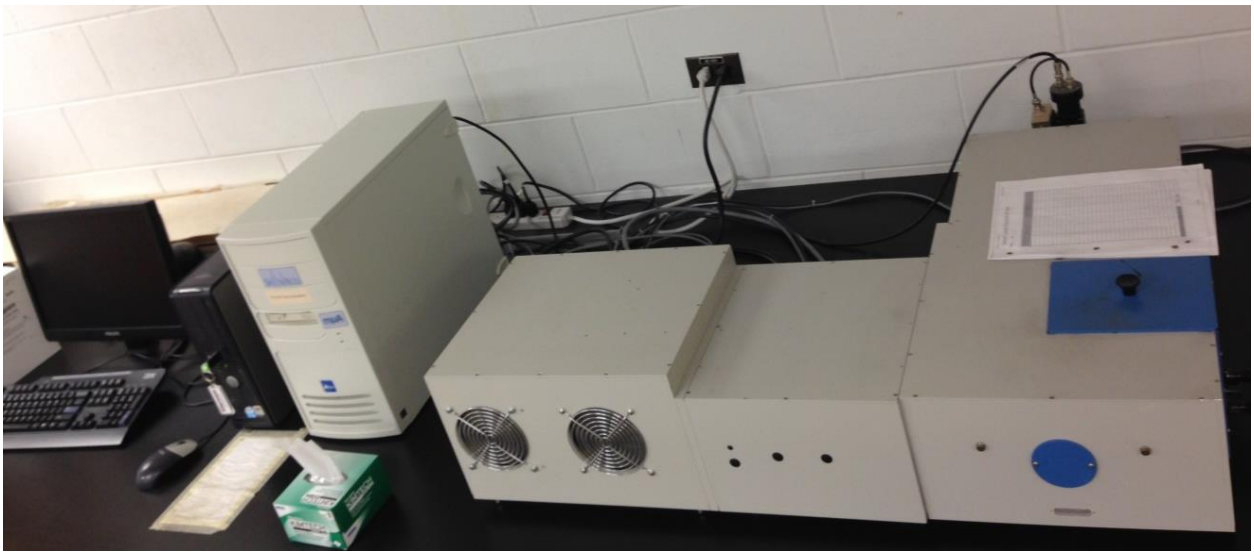

Figure 6.B, Photo of Fluorolog-3 Horiba Jobin Yvon Spectrofluorometer.

Fluorescence is a photoemission process where emission occurs when an electron has been promoted to an excited state by a photon from incident light and through molecular relaxation through a radiative pathway emits a photon while returning to the ground state[42]. Figure 7, a generic Jablonski diagram, shows the various electronic states of a fluorophore and transitions between them during absorption and emission of a photon. S_0 represents the singlet ground state energy level of a fluorophore while S_1 and S_2 represent the first and second singlet excited states respectively. Each of these excited states contain many closely spaced vibrational energy levels where the spacing is about 1500 cm^{-1}[37] as shown by the vibrational energy levels 0, 1, and 2 of the ground state S_0. An electron can be promoted from the ground state to an excited state after it has been excited by a photon from incident light as indicated by the blue and purple arrows which show the promotion of electrons to the second and first excited states respectively. An electron, once it has been excited, is promoted to one of the many vibrational energy levels of the excited states where it will then rapidly return to the lowest vibrational energy level of the first excited

state[42]. The return of the electron to the lowest vibrational energy level occurs through the rapid vibrational movement of the molecule which releases the excess energy of the electron in the form of heat[43] through a non-radiative pathway known as internal conversion as indicated by the black dashed lines. These Internal conversion processes typically occur on an extremely rapid time scale of 10^{-14} to 10^{-10} seconds[44].

Once an electron has returned to the lowest vibrational energy level of the first excited state it can return to the ground state through luminescence which is a radiative pathway that produces light as the electron decays back to the ground state. Luminescent pathways are typically favoured for the return of an electron to the ground state because of the large energy gaps between the excited and ground states of a molecule. The energy gaps between S_0 and S_1 are on the order of magnitude of 10000 cm^{-1} [42] which is much larger than the vibrational energy level gaps which are only 1500 cm^{-1}. When the electron returns to S_0 from S_1 *via* a non-radiative pathway the relaxation rates are 10^{-7} seconds - 10^{-5} seconds for a rigid molecule whereas radiative or luminescent pathways have relaxation rates ranging from 10^{-9} - 10^{-6} seconds[40,45].

Luminescence is broken down into two major mechanisms, fluorescence and phosphorescence. Phosphorescent decay occurs when an electron in the S_1 ground state undergoes Intersystem Crossing indicated by the solid black arrow. Intersystem Crossing is the mechanism by which an electron undergoes a spin conversion from the first singlet state S_1 to the first triplet state T_1. The return of an electron to the singlet ground state S_0 from a triplet state shown as the red downward arrows is forbidden which results in a very slow decay that is several orders of magnitude larger than the decay through fluorescence[40].

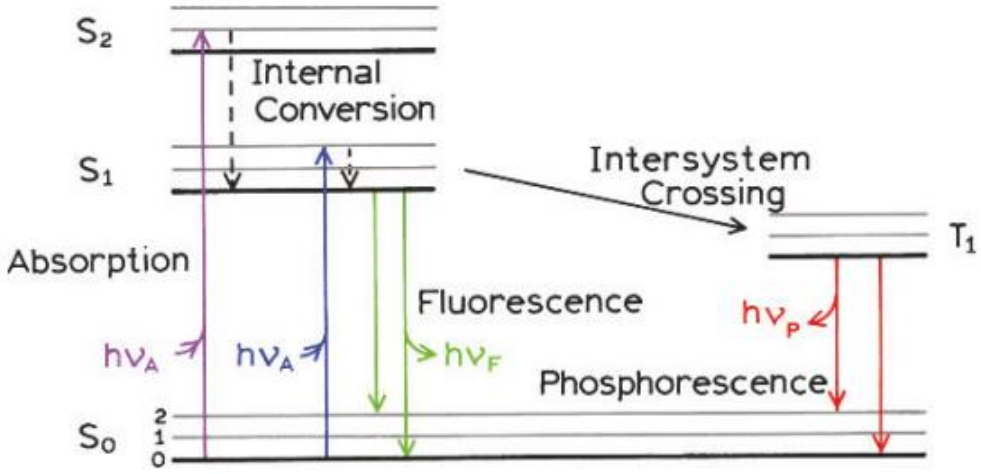

Figure 7. Generic Jablonski Diagram[40]

Fluorescence occurs when there is a transition of an electron from a singlet excited state back to a singlet ground state as shown by the green downward arrows[40]. According to the Pauli exclusion principle electrons in the same orbital cannot share the same quantum numbers. Thus, as shown in figure 8A, two electrons in the same orbital must have opposite spin quantum numbers represented by the up and down orientations of the arrows[46]. This is the case for electrons in the singlet state where all the electrons are paired with opposite spins. If the spin of the electron remains in a singlet state during the transition from the ground state to the excited state as seen in figure 8*B* the transition back to the ground state is spin allowed and can happen very quickly by the emission of a photon in the form of fluorescence light[46] which is why fluorescent transitions are typically favoured for the larger energy gaps found between the excited and ground states.

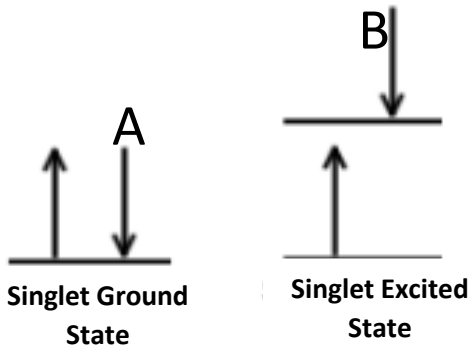

Figure 8. Paired electron spins in the ground state (A) and electrons spins in the excited state (B)[43]

When an electron returns to the ground state and produces fluorescence an important parameter the fluorescence quantum yield can be measured. The quantum yield is the ratio of photons emitted vs photon absorbed[47]. A molecule with a high quantum yield will be more efficient when converting a higher proportion of the exciting light to emitted light. The efficiency of the conversion and consequently the quantum yield is affected by the amount of fluorescent light produced as the electron returns to the ground state but additionally by how much energy is released in a non radiative pathway where this relationship is shown in Figure 9.

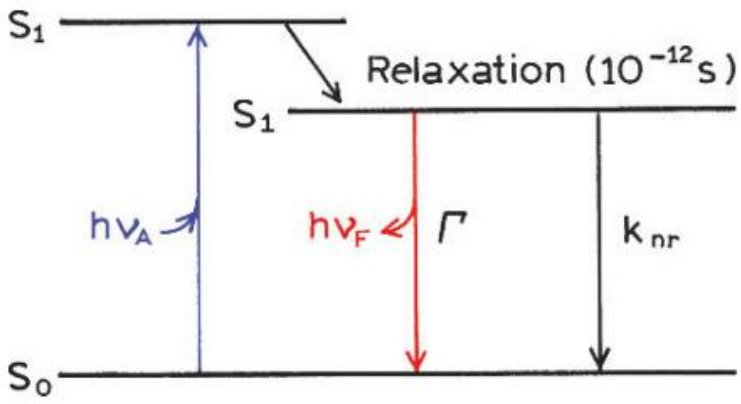

Figure 9. Jablonski diagram that focuses on the decay of an electron from the lowest vibration energy levels of the first singlet excited state to the singlet ground state. Γ represents fluorescent decay while k_{nr} represents non-radiative decay[40].

The excited electron can return to the ground state through a combination of Γ which represents the emissive rate of the fluorophore and k_{nr} which is the rate of non radiative decay where this relationship can be better understood by equation 1[40]. The quantum yield Q can reach values close to 1 if there is almost no non-radiative decay and be near 0 if there is almost no fluorescence where most of the decay originates from a non-radiative method[48].

Equation 1. $Q = \frac{\Gamma}{\Gamma + k_{nr}}$

Beyond non-radiative decay the quantum yield can be decreased through fluorescence quenching[42]. Fluorescence quenching can occur through a variety of mechanisms such as collisional quenching where the excited state of a molecule is deactivated when it interacts with

another molecule or through static quenching complexes where a fluorophore forms a bond with a molecule that disrupts the grounds state excitation of the fluorophore[40].

1.8 Molecular Probes

Small molecule fluorescent probes are useful tools designed to study cell biology, drugs, detect environmental contaminants, and further the detection of cancer. These probes are molecules that can change their fluorescence quantum yield in response to binding to other molecules, chemical reactions, or changes in their environment. They can be designed to control many intrinsic characteristics including emission wavelengths, binding affinities, and even subcellular localization[49]. To study ScOTU1 dynamics two fluorescent probes will be utilized, Ubiquitin-Rhodamine and Bis-ANS.

1.8.1 Ubiquitin Rhodamine

In our enzyme activity assays a substrate known as ubiquitin rhodamine 110 was used. Rhodamines are a type of fluorescent probe that have a fluorescent quantum yield near unity[40]. Additionally rhodamine fluorophores are not sensitive to solvent polarity and they have extremely high molar extinction coefficients. These factors make rhodamine fluorophores very sensitive to detection. Ubiquitin-Rhodamine 110 is composed of a ubiquitin molecule covalently linked to a rhodamine fluorophore through a linker RLGG amino acid sequence that mimics the naturally occurring iso-peptide bond to an ε-amino group of a lysine residue of a ubiquitinated protein that OTU1 recognizes and cleaves in an endogenous ubiquitin polymer[50,51]. When bound to ubiquitin the fluorescence of rhodamine is completely quenched but when the linker region has been cleaved the free rhodamine can fluoresce in solution as shown in Figure 10 which makes it an ideal fluorescent probe to monitor the enzymatic activity of ScOUT1.

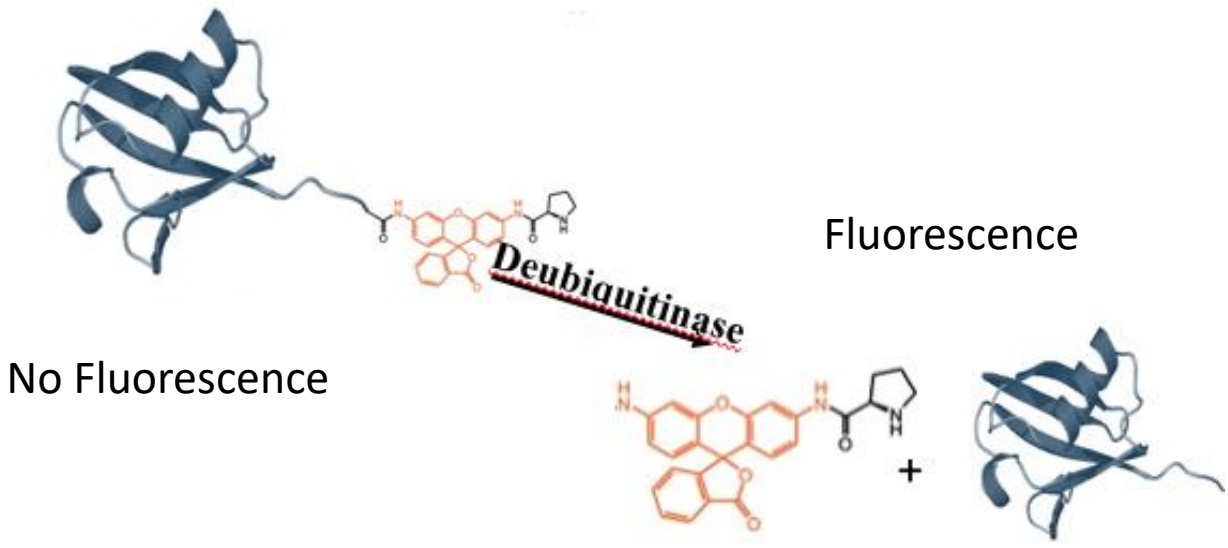

Figure 10. Mechanistic description of the cleavage of the linker region between rhodamine (orange) and ubiquitin (blue) by deubiqutinases which results in an increase in fluorescence[52].

1.8.2 Bis-ANS

Bis-ANS is a hydrophobic surface probe which is defined as a molecule with extrinsic fluorescence that can bind reversibly or irreversibly to hydrophobic regions on a protein's surface[48]. Hydrophobic probes have been used for many facets of protein characterization such as protein-surfactant interactions, aggregation and fibrillation properties, and most importantly with regards to OTU1, to monitor conformational changes by assessing changes in surface hydrophobicity[48]. Other examples of hydrophobic probes include ANS, cis-parinaric acid, and 2-p-toluidinylnaphthalene-6- sulfonate (TNS). Most hydrophobic probes share the following properties: when the hydrophobic probe is free in an aqueous solution its fluorescence quantum yield is very low; once the probe is in a nonpolar viscous environment, its fluorescence quantum yield increases significantly[53]

The chemical structure of bis-ANS is given in Figure 11. This molecule has the following two functional groups: the fluorescent naphthyl and the electron donating aniline. Once the naphthyl group is photoexcited, the aniline group can twist into the correct geometry, donate an electron to the excited naphthalene moiety and form a twisted internal charge transfer (TICT) state[48] which alters the electronic energy levels as shown in Figure 12. The formation of a TICT state is a non-radiative process and decreases the fluorescence quantum yield of bis-ANS[48]. The rate of TICT state formation is dependent on two environmental parameters[48]: a) solvent polarity; TICT state formation increases with solvent polarity; b) solvent viscosity; increasing viscosity prevents the twisting of the aniline group and impedes TICT state formation.

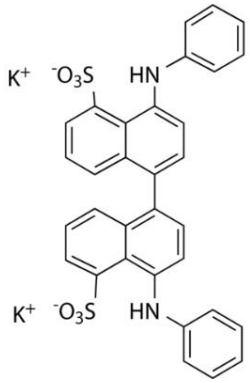

Figure 11. Structure of Bis-ANS which shows the closely spaced amino and aromatic group.[54]

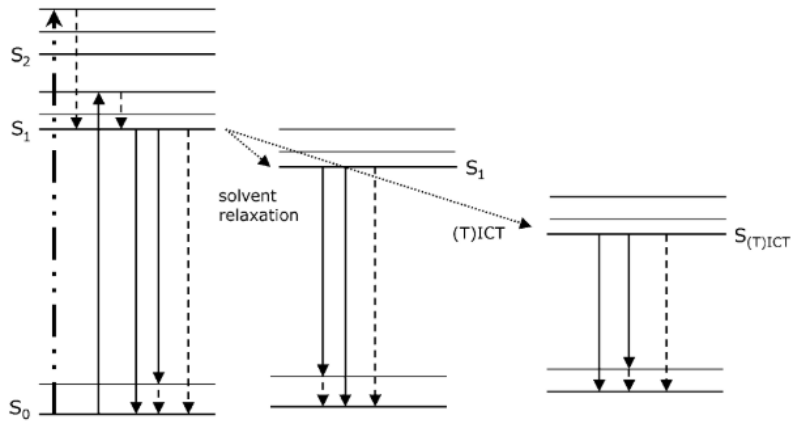

Figure 12. Jablonski Diagram exhibiting the effects of Solvent Relaxation and Twisted Intramolecular Charge Transfer Interactions on electronic energy levels[48]***.*** *The electron is excited by a photon represented by the dashed and dotted arrow. The excited electron returns to the first vibrational energy level of S_1 through non-radiative pathways (Dashed lines). Once there, the electron will fluoresce returning to the ground state S_0 (Solid lines).*

When a protein is present in solution the hydrophobic regions on bis-ANS such as the aromatic rings can now associate with the hydrophobic patches on the surface of the protein (i.e., binds non-covalently to a hydrophobic surface through a combination of electrostatic interactions, the hydrophobic effect, and Van der Waals forces. The association lowers the local polarity experienced by the probe and inhibits bis-ANS twisting required to produce the TICT state[55]**.** These two-protein binding-induced changes in the probe microenvironment[56], greatly increase the quantum yield of bis-ANS causing a large increase in fluorescence. This relationship between solvent polarity and viscosity and fluorescence quantum yield are shown in Figure 13, where the fluorescence of bis-ANS is shown in solvents of varying polarity and viscosity.

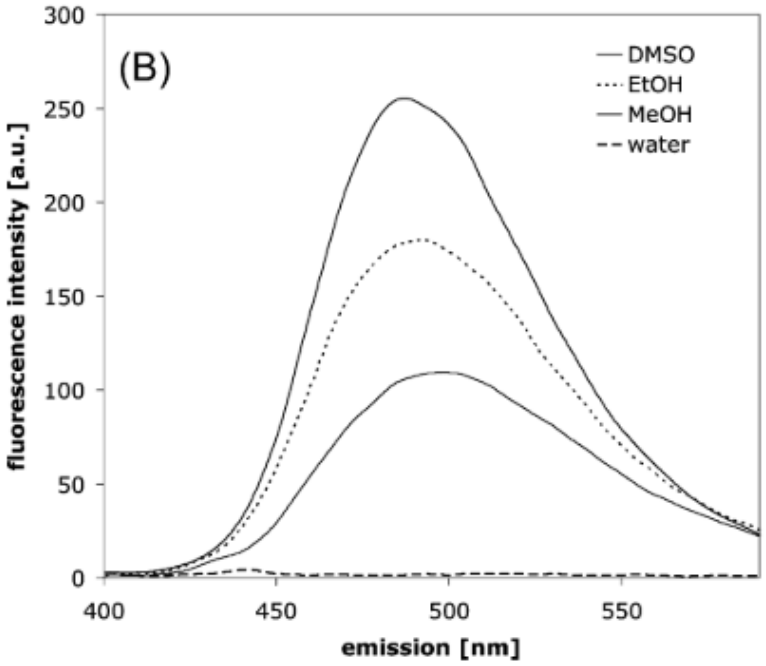

Figure 13. 1 μM Bis-ANS in solutions of varying polarity and viscosity. [48]

Bis-ANS in a solvent consisting of water as indicated by the lowest dashed line has almost no fluorescence. This quenching of fluorescence occurs because water is a polar solution with a dielectric constant of 80.4[57] meaning that it produces a significant amount of solvent relaxation. Bis-ANS in a solution of methanol which has a dielectric constant of 33[57] fluoresces more due to a decrease in solvent polarity and the trend continues with ethanol which has a dielectric constant of 25.3[57] and a continued increase in fluorescence quantum yield. Dimethyl sulfoxide (DMSO) though, has a dielectric constant of 47.24[58] which is higher than either methanol or ethanol but despite the increased solvent polarity DMSO but has the largest quantum yield. The reason Bis-ANS has the greatest fluorescence quantum yield in a solvent of DMSO is based on relative solvent viscosity and not polarity. DMSO has a solvent viscosity of 1.987[58] which is significantly larger than that of ethanol, methanol and water with values of 1.04, 0.54, and 0.89 respectively[59].

Viscosity plays a role in fluorescence quantum yield because in a more viscous environment non radiative pathways which rely significantly on vibrational movements are dampened which favours a radiative decay of the electron and subsequent fluorescence.

1.9 pH Dependent Conformational Changes

To assess if there are pH-dependent conformational changes occurring within ScOTU1 a Bis-ANS based experiment was used as it has been shown to be an ideal probe with which to measure pH-dependent conformational changes of a variety of proteins[60]. The cleft that contains the catalytic triad of the ScOTU1 domain is a hydrophobic region and so bis-ANS can be used to assess the accessibility of the cleft as the pH is varied[61].

1.10 Goals of the Research

The goals of this research are to study the conformational dynamics that occur in the ScOTU1 catalytic domain of the enzyme OTU1 from yeast *Saccoromyces cerevisiae.* The pH dependence of bis-ANS fluorescence will be studied in addition to experiments directly measuring the pH dependence of catalysis using Ubiquitin Rhodamine. These experiments will allow insight into the catalytic mechanism of ScOTU1 by revealing if catalysis occurs through a one state mechanism where the ubiquitin molecule binds and then catalysis occurs or through a two-state mechanism where a conformational change must first occur within the free enzyme and subsequently the ubiquitin binds.

Chapter 2

Materials and Methods

2.1 Materials

Lysogeny Broth (LB) powder and RNase A solution were purchased from BioBasic. Tris(hydroxymethyl)aminomethane hydrochloride (TRIS-HCl), sodium chloride, and sodium phosphate dibasic were purchased from Fisher Chemical. Dithiothreitol (DTT), isopropyl-B-D-thiogalactopyranoside (IPTG), and tris(2-carboxythyl)phosphine (TCEP) were purchased from GoldBio. DNase, lysozyme, and 4,4'-Dianilino-1,1'-Binapthyl-5,5'Disulfonic Acid (Bis-ANS) were purchased from Sigma-Aldrich. Kanamycin was purchased from Fisher Bioreagents. Magnesium sulfate was purchased from Mallinckrodt. Imidazole and glycerol were purchased from Fisher Scientific. Ni-NTA Agarose was purchased from Qiagen and ubiquitin-rhodamine was purchased from Boston Biochem.

2.2 Methods

2.2.1 Preparation of ScOTU1

a) Glycerol Stock Preparation

A plasmid for the 6xHis tag ScOTU1 protein was provided by the laboratory of Professor Brian Mark (Department of Microbiology at the University of Manitoba). The plasmid was transformed into *E. coli* BL21-Gold DE3 cells (GoldBio) by chemical transformation. The cells were plated on agar plates and the colonies were selected by the degree of their growth after overnight incubation at 37 °C. One colony was used to inoculate a 25 ml starting culture in a 125 ml baffled Erlenmeyer flask. The solution was comprised of 30 µg/ml of kanamycin, 2 µM of $MgSO_4$, and 25 mg/L of LB media (Growth Mix[1]) at pH 7. The starting culture was shaken overnight at 37 °C and 300

RPM. This starting culture was mixed with glycerol to make a 20% glycerol solution used as the progenitor of future ScOTU1 preparations.

b) ScOTU1 Overexpression

A glycerol stock containing *E. coli* ScOTU1 BL21 cells was used to inoculate a 25 ml LB broth starting culture in a 125 ml baffled Erlenmeyer flask. The Growth Mix[1] starting culture was shaken overnight at 37 °C and 300 RPM. 2 ml of the starting culture was used to inoculate a 2 L baffled Erlenmeyer flask containing 400 ml of Growth Mix[1]. The overexpression culture was grown for 3.5 hours at 37 °C and 190 RPM until it reached an OD_{600nm} between 0.6-0.8 when it was induced with 1 µM IPTG and allowed to shake overnight. The overexpression culture was centrifuged at 4 °C in a 1 L bottle for 20 minutes at 6000 RPM and frozen in a -80 °C freezer.

c) ScOTU1 Purification

The frozen cell pellet was resuspended in a pH 8 lysis buffer consisting of 50 mM TRIS-HCl, 300 mM NaCl, and 2 mM TCEP. Cells were lysed using a freeze-thaw method that renders *E. coli* cells susceptible to lysosomal degradation by physically fracturing the cell walls through repeated freeze-thaw cycles. This method of cell lysis typically results in a greater and more consistent protein yield than conventional methods like French press or sonication[57]. 5 ml of a 5 mg/ml solution of lysozyme was prepared in lysis buffer and was added to the resuspended pellet. The suspended cells were then equilibrated at 4 °C in a cold room for 30 minutes. After 30 minutes the cell resuspension was gently stirred on a stir plate in a cold room for 10 minutes after which a small amount of DNase and RNase were added to the mixture and gently stirred again for 10 minutes. The cell resuspension solution was then refrozen in a -80 °C freezer for 45 minutes. With the first cycle complete the entire procedure was repeated twice more for a total of 3 freeze-thaw

cycles. Once all the freeze-thaw cycles were completed the cells were centrifuged for 1 hour at 14500 RPM for 45 minutes at 4 °C.

The crude lysate was applied to a Ni-NTA agarose gravity chromatography column to separate the His-tagged ScOTU1 protein from DNA, RNA, and other macromolecule contaminants. The column was washed with ten column volumes of imidazole at increasing concentrations of 12.5 mM, 25 mM, and 250 mM respectively. The 250 mM imidazole solution eluted the protein from the column and 2 mL of this protein solution was collected and was injected onto a Superdex 75 10/300 GL size-exclusion column that had a length of 30 cm and inner diameter of 10 mm (GE Healthcare) to separate any aggregates or contaminants from the ScOTU1 protein. The purified protein was flash frozen in small volumes using liquid nitrogen and then stored in a -80 °C freezer for later use.

2.2.2 Bis-ANS Hydrophobic Surface Study

Bis-ANS experiments were modified from a literature procedure[61]. The preparation of stock Bis-ANS was done by dissolving Bis-ANS in buffers with pH values ranging from 6 to 9 consisting of 50 mM sodium phosphate dibasic and 50 mM sodium chloride (Bis-buffer). The target concentration of the stock Bis-ANS solutions was 200 µM which was obtained by measuring the absorbance of the solutions in a Helios Zeta UV-VIS spectrophotometer (Thermo Scientific) at 385 nm and using a 16,790 $M^{-1}cm^{-1}$ extinction coefficient. The working Bis-ANS concentrations ranged from 2.5-80 µM for a total of nine experiments done in triplicate at each pH value.

Frozen protein was thawed to room temperature and protein absorbances were measured at 280 nm using a Nanodrop 2000s spectrophotometer (Thermo Scientific) and a 160 mM stock solution of DTT was prepared in Bis-buffer[2]. The final working concentrations of ScOTU1 and DTT in the semi micro cuvettes were 0.5 µM and 2 mM respectively. Twenty-seven microfuge tubes

containing the appropriate amount of Bis-ANS, ScOTU1, and DTT were all prepared and were thoroughly mixed (Pressure Mixer) and left in a 4°C refrigerator for 1 hour to allow for complete binding.

The microfuge tubes equilibrated to room temperature for 10 minutes after the hour incubation time elapsed. A Jobin-Yvon Fluorolog fluorescence spectrometer (Horiba) was used to record the spectrum of the solutions using an excitation wavelength of 350 nm and an emission wavelength range of 450–530 nm. The emission and excitation slit widths were set to 2 nm and all the experiments were done in a 10 mm by 3.5 mm quartz cuvette (Starna Cells) with a 0.4 mm pathlength. The fluorescence of free Bis-ANS and DTT was subtracted for the measured data points in addition to a correction that was made for the fluorescence of the solutions caused by inner filter effects.

When Bis-ANS binds to hydrophobic patches on proteins there is an increase in the fluorescence quantum yield. Augmentation of fluorescence as Bis-ANS concentration is increased follows a sigmoidal distribution which typically indicates some cooperativity in the binding event [63]. To assess the extent of the apparent cooperativity and the percentage of Bis-ANS bound over the pH ranges studied a Hill equation was chosen to fit the sigmoidal data.

The Hill equation is represented in equation 1. The *n* variable is the Hill coefficient. The Hill coefficient quantifies the degree of cooperativity of a sigmoidal curve; if the *n* value is less than one the system does not exhibit cooperativity but if there is cooperativity the coefficient is greater than one[64]. K_d is the apparent dissociation constant and X is the ligand concentration.

$$Eq\ 2.\quad y = \frac{[X]^n}{K_d + [X]^n}$$

Using equation 2 it is possible to determine if the binding is cooperative and additionally the Hill equation can be used to determine if there is a change in the percentage of Bis-ANS bound to the protein depending on the pH of the solution. To determine the percentage of Bis-ANS bound to the protein a slightly modified version of the Hill equation is used which includes the parameters y_0 and a as shown in equation 3.

$$Eq\ 3.\quad y = y_0 + \frac{a[X]^n}{K_d + [X]^n}$$

The a variable represents the maximum response for a particular amount of Bis-ANS added and y_0 is the minimum response[65]. To determine the maximum amount of fluorescence possible (y) the ligand concentration [X] is set to infinity and the modified Hill equation is then equation 4 where (y_{max}) is the maximum fluorescence after adding an infinite amount of Bis-ANS.

$$Eq\ 4.\quad y_{max} = y_0 + a$$

Fitting the sigmoidal curves to equation 4 as seen in Figure 14 it is possible to find both the maximum fluorescence value y_{max} and the minimal value y_0 and with those two parameters the percentage bound is calculated using equation 5, where y_{exp} is the measured fluorescence for each experiment.

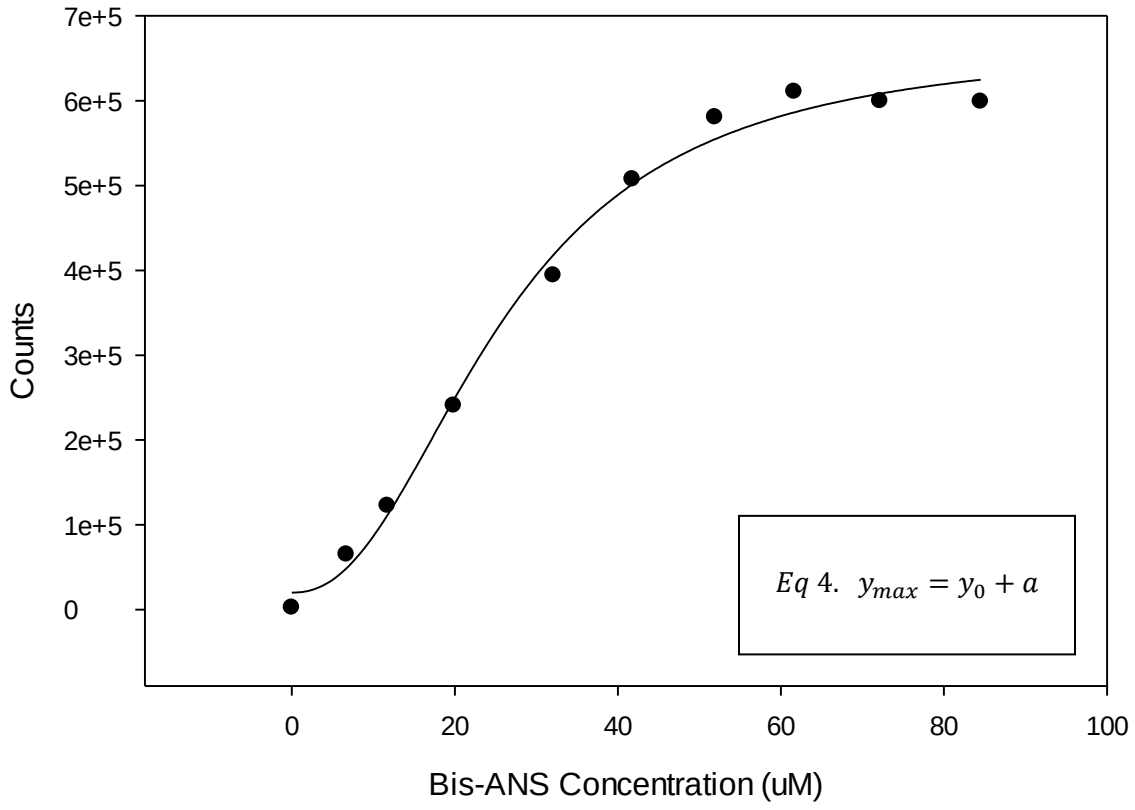

Figure 14. Binding curve of Bis-ANS at pH 9 with 0.5 µM ScOTU1 and 2 mM DTT in Bis-Buffer[2] where counts represent the uncalibrated measurement of photons incident on the detector.

$$Eq\ 5.\ \ Percentage\ Bound = \frac{y_{exp} - y_0}{y_{max} - y_0}$$

Using the calculated percentage bound values, it is possible to create a percentage bound vs concentration plot that can be fit by the three parameter Hill equation, equation 2 where it is possible to determine the dissociation constant K_d which is a direct measure of the binding efficiency.

2.2.3 Ubiquitin Rhodamine Deubiquitinase Study

Ubiquitin Rhodamine experiments were modified from the literature[50]. Deubiquitinase experiments were performed in a total volume of 850 µl in a 1 ml semi-micro cuvette in a buffer consisting of 50 mM TRIS-HCl, 50 mM NaCl, and 2 mM DTT (ContBuffer[3]) with pH values ranging from 6 - 7.5. ScOTU1 and Ubiqutin-Rhodamine working concentrations were 50 nM and 250 nM. The mixture was incubated at 4°C for 1 hour and allowed to equilibrate to room temperature for 10 minutes before experiments began. A Jobin-Yvon Fluorolog fluorescence spectrometer (Horiba) was used to record the spectra of the solutions over the course of 1 hour using an excitation wavelength of 485 nm and an emission wavelength of 535 nm. The emission and excitation slit widths were set to 2 nm respectively and all the experiments were done in a 10 mm by 3.5 mm quartz cuvette (Starna Cells) with a 1 cm pathlength. The fluorescence of free Ubiquitin-Rhodamine and DTT was subtracted for the measured data points and corrected for inner filter effects.

The cleavage of Ubiquitin-Rhodamine by ScOTU1 follows Michaelis-Menten kinetics[19] and due to that it is possible to modify the basic Michaelis-Menten reaction scheme as shown in equation 6. [P] is the concentration of free rhodamine as the reaction progresses, $[e_0]$ is the initial enzyme concentration, [S] is the substrate concentration, K_M is the Michaelis constant and it is the concentration of substrate required to reach half of the maximum conversion rate, and k_{cat} is the turnover number and it represents the number of substrate molecules converted per time.

If it is assumed that K_m is much greater than the concentration of the substrate at any moment equation 6 can be simplified to equation 7. The assumption is reasonable because of the low working concentration of substrate and its steady decrease as the experiment proceeds.

Eq 6. $\frac{d[P]}{dt} = \frac{k_{cat}[e_0][S]}{K_M+[S]}$

Eq 7. $\frac{d[P]}{dt} = (\frac{k_{cat}}{K_M})app[e_0][S]$ where $\left(\frac{k_{cat}}{K_M}\right)app = (\frac{k_{cat}}{K_M})\frac{1}{\frac{[H]}{K_{E1}}+1+\frac{K_{E2}}{[H]}}$

Equation 7 represent the rate of appearance of free rhodamine from Ubiquitin-Rhodamine after cleavage by ScOTU1. k_{cat}/K_m is the specificity constant and it is a quantity that provides a measure of the efficiency of an enzyme for a substrate under different conditions which in this experiment is alteration of pH. The apparent k_{cat}/K_m takes into consideration the changes in the hydrogen ion concentration which is a direct measure of the pH of the solution.

To fit this equation to the experimental data equation 7 is integrated with respect to time which results in equation 8.

Eq 8. $P = S_0(1 - e^{\left(\frac{k_{cat}}{K_M}\right)app[e_0]t})$

Equation 8 then undergoes a Taylor series expansion which provides an approximation for the value of a function at a particular time[66]**.** This approximation simplifies the fitting of the data to a simple polynomial equation as shown in equation 9.

Eq 9. $F = at + bt^2$

Where $at = -\left(\frac{k_{cat}}{K_M}\right)_{app}[e_0]t$ & $bt^2 = -\{\left(\frac{k_{cat}}{K_M}\right)_{app}\}^2\frac{[e_0]^2t^2}{2}$

Simplifying equation 9 by dividing bt^2 by at results in Eq. 10

Eq 10. $\frac{bt^2}{at} = \frac{-\{\left(\frac{k_{cat}}{K_M}\right)_{app}\}^2\frac{[e_0]^2t^2}{2}}{-\left(\frac{k_{cat}}{K_M}\right)_{app}[e_0]t} = \left(\frac{k_{cat}}{K_M}\right)_{app}\frac{[e_0]}{2}t$

Calculating $(k_{cat}/K_m)_{app}$ is a straightforward process for solving for one unknown as the initial enzyme concentration is always known.

Chapter 3

Results

To study the pH-dependent properties of ScOTU1 a Ubiquitin-Rhodamine substrate was used in addition to Bis-ANS a hydrophobic surface probe. Ubiquitin-Rhodamine experiments were applied to determine if electrostatic interactions between ubiquitin and ScOTU1 might stabilize the active conformation of the enzyme thereby providing access to the catalytic triad within the active site at a wide range of pH values. Bis-ANS experiments were used to assess if there were conformational changes that occurred within ScOTU1 as the pH was altered by measuring the amount of Bis-ANS fluorescence at different pH values and subsequently determining the binding constant $K_{d.}$

3.1.1 Protein Precipitation

During the dialysis portion of the protein purification there was recurrent aggregation of ScOTU1 which greatly decreased the yield of protein. The purpose of dialysing ScOTU1 once it had eluted from the nickel column was to perform a buffer exchange to reduce the high salt and TRIS-HCl concentration of the lysis buffer to match the lower concentrations of salt and TRIS-HCl in the buffers used to perform experiments. Additionally, dialysis was used remove small molecules such as imidazole which was used to elute the protein from the nickel column. Precipitation can occur during the course of dialysis if the protein is unstable at the dialysis temperature or unstable at the lower salt concentrations especially if the salt concentration is dropped rapidly[67]. Additionally, the protein might precipitate if nickel ions from the column resin leach into the buffer causing the

coordination of the histidine tag on multiple proteins to form complexes that cause the protein to precipitate out of solution[68].

The initial dialysis procedure from Roy Hutchings[39] consisted of dialyzing the protein overnight at 4 °C in 1 L of 25 mM TRIS-HCl, 150 mM NaCl, 2 mM DTT at pH 8.0 using a 2 kDa pore size dialysis membrane (Spectrum Labs).

The first strategy employed to reduce protein precipitation was to perform the entirety of the protein purification through a nickel column in a 4 °C cold room. The protein may not have been stable at room temperature and therefore may have been denaturing during a 2-hour period at room temperature as it was passed through the nickel column and washed with buffers during the purification phase. After multiple trials using this new strategy there remained a significant amount of protein precipitation after dialysis was complete.

The next strategies employed focused on directly modifying the dialysis procedure to address the possible issues previously listed. The first issue addressed was that of the rapid salt decrease. The protein was initially in a lysis buffer consisting of 50 mM TRIS-HCl, 300 mM NaCl, and 2 mM DTT at pH 8.0 and so a sudden decrease to the dialysis solution concentrations could result in an unstable protein. The affect that salt concentration can have on protein stability during dialysis is not completely understood and is greatly dependent on the ionic interactions within a protein and often it is through trial and error that the correct ionic strength can be determined for the protein. When the salt concentration is lowered, electrostatic shielding weakens ionic attractions or repulsions and at higher salt concentrations electrostatic shielding is saturated which alters a protein's hydrophobic interactions[67]**.** To minimize the steep drop in salt concentration the dialysis was initially done in a two-step fashion by slowly lowering the salt concentration from the lysis buffer composition to that of the final dialysis buffer over the course of 6 hours. The first dialysis

buffer solution consisted of 30 mM TRIS-HCl, 250 mM NaCl, at pH 8.0, the second dialysis buffer was 25 mM TRIS-HCl, 200 mM NaCl, at pH 8.0, and the final solution was 25 mM Tris-HCl, 150 mM NaCl at pH 8.0 as indicated in table 1.

Table 1. Dialysis buffer composition at different time intervals

Dialysis Buffer Composition	**Time Dialyzed in Buffer (hours)**
30 mM TRIS-HCl, 250 mM NaCl, at pH 8.0	2 hours
25 mM TRIS-HCl, 200 mM NaCl, at pH 8.0	2 hours
25 mM TRIS-HCl, 150 mM NaCl at pH 8.0	Overnight

At the end of the overnight dialysis in the final buffer precipitation still occurred in the solution. To try to remedy this problem the final overnight dialysis was shortened to last only 6 hours but even at the end of that time interval there was observed precipitation of the protein.

Ethylenediaminetetraacetic acid (EDTA), a chelating agent, forms a stable complex with nickel ions found in the dialysis solution[69] and so the goal of this portion of the research was to see if adding EDTA to solution could reduce the concentration of free nickel ions in the dialysis buffer which might reduce the precipitation of ScOTU1 possibly due to nickel ions in solution. The first two solutions in Table 1 were modified as shown in Table 2 to include 5 mM EDTA. Once again after the overnight trial precipitation was found in the dialysis tubing and again the final overnight dialysis was shortened to 6 hours but even then, precipitation still occurred.

Table 2. Dialysis buffer composition including EDTA at different time intervals

Dialysis Buffer Composition	**Time Dialyzed in Buffer (hours)**
30 mM TRIS-HCl, 250 mM NaCl, 5 mM EDTA at pH 8.0	2 hours
25 mM TRIS-HCl, 200 mM NaCl, 5 mM EDTA at pH 8.0	2 hours
25 mM TRIS-HCl, 150 mM NaCl at pH 8.0	Overnight

The last test experiment that was carried out consisted of altering the pH of the buffer to see if increasing or decreasing the pH would allow it to be more stable in solution. The isoelectric point of ScOTU1 was calculated to be 4.82 after I inserted the protein sequence into Bioinformatics Resource Portal ExPASy. When the pH of a solution matches the isoelectric point of a protein it means that the protein is typically minimally soluble[70]. The pH of the dialysis in each experiment was 8 but there may have been deprotonation at pH 8 that might alter the protein structure, so the buffer was adjusted to pH 7.5 and the experiments in Tables 1 and 2 were repeated. Despite all the changes, precipitation continued to occur during dialysis and resulted in a large decrease of protein yields.

After attempting to solve the precipitation due to dialysis for an extended period, the dialysis step of the purification was eventually removed and instead the protein was directly injected onto a Superdex 75 size exclusion column. With the dialysis step replaced by a rapid buffer exchange using the Superdex 75 column no precipitation was observed, and contaminants were removed as shown by Figure 15, the elution profile of the protein using the column. This rapid exchange most

likely worked because the protein was kept in solution for 1.5 hours during the buffer exchange rather than the 14 hour incubation times that were used with dialysis. The protein may not have been stable enough to remain in solution for an extended period and shortening the exchange time kept the protein from degrading or unfolding.

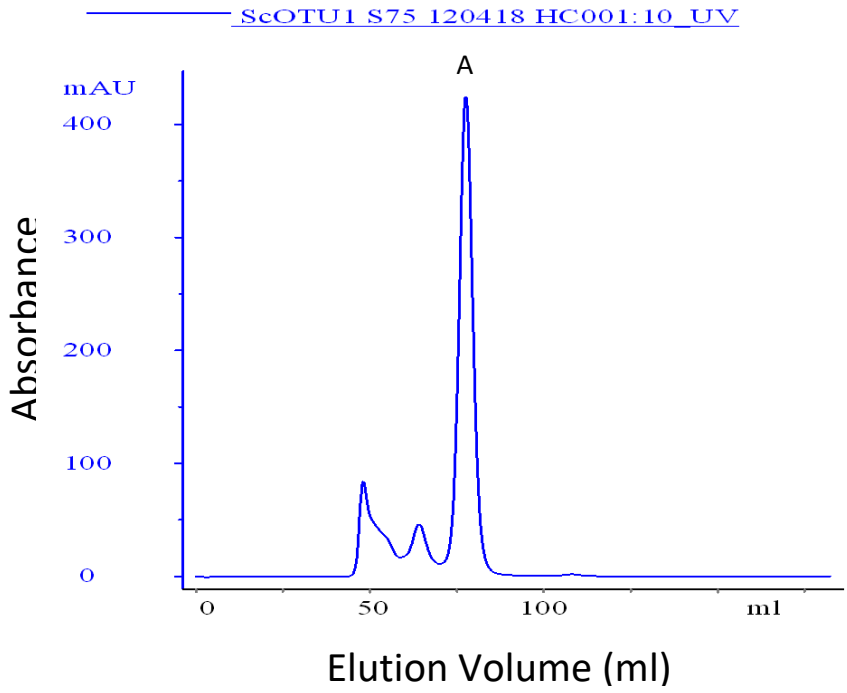

Figure 15. ScOTU1 elution profile using a Superdex 75 size-exclusion column where peak ***(A)*** *represents the eluted protein. Elution buffer consisted of 25 mM TRIS-HCl, 150 mM NaCl, and pH 8.0 buffer with fraction volumes of 1 mL*

3.1.2 Protein Yield

The protein yield of ScOTU1 using LB broth when dialysis was still used during protein purification was on average 6 mg/L. After the purification was optimized by the replacement of

protein dialysis with a rapid buffer exchange the protein yield increased to an average of 13.4 mg/L. Alternative *E. coli* growth media have been shown to be more efficient than LB broth when growing cells and one such growth media is auto-inducing media. Auto-inducing media have been shown to increase cell culture density and the concentration of protein per volume of culture when compared to traditional media like LB broth[71]. The decrease in cell density and protein yield is driven by the fact that in IPTG-inducible systems unintended induction can occur as the cells reach saturation due to the presence of lactose in the media from enzymatic digests of casein which are commonly found in media such as LB broth which results in a decrease in cell density and consequently protein yield. Lactose in the system can be taken up by the cells and converted to the inducer allolactose which can bind to the lac repressor and consequently allow expression of the protein[72].

Auto-inducing media circumvent this issue by incorporating compounds that inhibit lactose induction but are depleted as cell growth continues such as amino acids and molecules like glucose in addition to specific growth conditions which specify high aeration and low temperatures. The conditions taken together result in cells achieving a higher culture density and subsequently higher protein yields. Using the fact that these amino acids and glucose are depleted as the cells grow Studier et al. (2005) were able to design media that enabled cell growth to much higher densities due to the gradual decrease of the inhibitory molecules which would then allow lactose to be taken up and metabolized which resulted in the start of induction and protein expression. A low phosphate isotope-labelling autoinducing minimal medium from the literature named LS- 5052 with a composition as shown in Table 3[72] utilized glucose as an inhibitor of induction by blocking the uptake and breakdown of lactose[73]. The LS-5052 medium was used to grow ScOTU1 cells to observe if protein yields would increase resulting in a more efficient protein growth system but

the yields using auto-inducing media and rich media were similar as shown in Table 4. It should be noted that there can be a large decrease in protein yield when using minimal media and despite that the yields of the rich and minimal media are very similar.

Table 3. Composition of auto-inducing media LS-5052 used to grow ScOTU1 culture

LS-5052 Composition
12.5 mM Na_2HPO_4
12.5 mM KH_2PO_4
50 mM NH_4Cl
5 mM Na_2SO_4
2 mM MgSO4
10 µM Fe + 9
54 mM Glycerol
2.8 mM Glucose
5.6 mM α-lactose
20 mM Succinate

Table 4. Protein yield of ScOTU1 using rich and autoinducing media lysosomal broth and auto-inducing media respectively.

Media	Protein Yield mg/L of culture
Lysosomal broth – Rich media	13 mg/L
LS-5052 media- Auto-inducing media	12 mg/L

3.1.3 Protein Purity

The purity of the eluted protein was assessed using sodium dodecyl sulfate–polyacrylamide gel electrophoresis (SDS-PAGE). As shown in Figure 16, two bands appeared on the gel at approximately 20 kDa and 40 kDa. The 20 kDa band is the appropriate molecular weight for ScOTU1 protein but the 40 kDa band most likely represented a disulphide-linked dimer of ScOTU1 that was not completely reduced through the addition of DTT

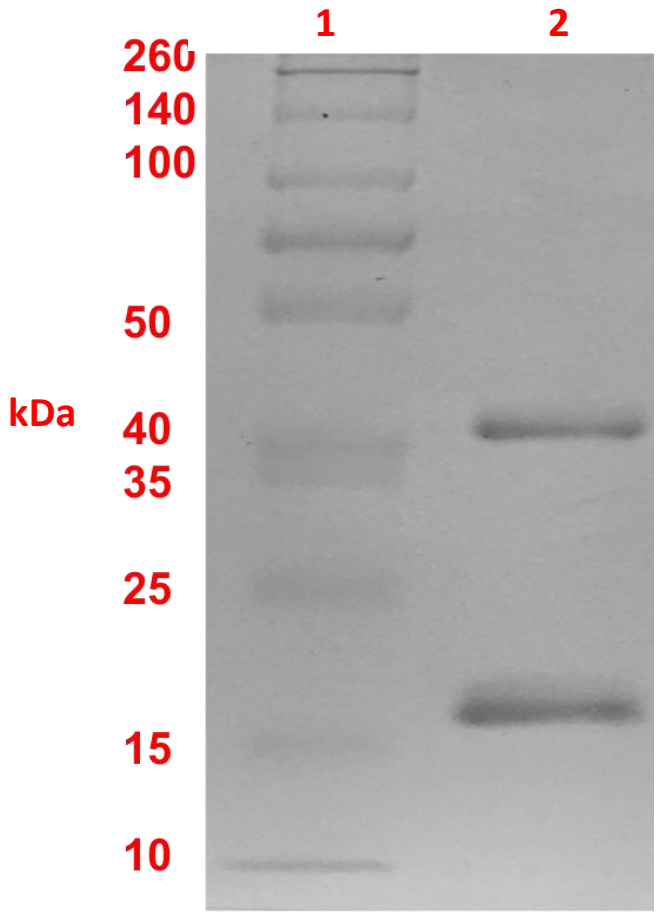

Figure 16. SDS-PAGE image of purified ScOTU1. Lane 1 represents the protein molecular weight standards (PageRuler Plus Prestained Protein Ladder, ThermoFisher Scientific) and lane 2 represents the eluted protein sample from the size exclusion column containing 2 mM DTT.

3.2 Ubiquitin-Rhodamine Deubiquitinase Experiments

Figure 17 is a reaction progress curve that shows a steady increase in fluorescence as time proceeds for the cleavage of Ubiquitin-Rhodamine by ScOTU1. This figure shows that ScOTU1 can recognize and cleave the RLGG amino acid sequence in the linker region between the ubiquitin and rhodamine portions of the substrate and confirms that the protein was correctly over-expressed, purified, and active. Another point is that at pH 7.0 there is enzyme activity which is

quantified with the specificity constant of 2180 $M^{-1}s^{-1}$ which was calculated based on the fit of the curve (Blue line) to equation 8 in the Materials and Methods section which is represented by the (Black line).

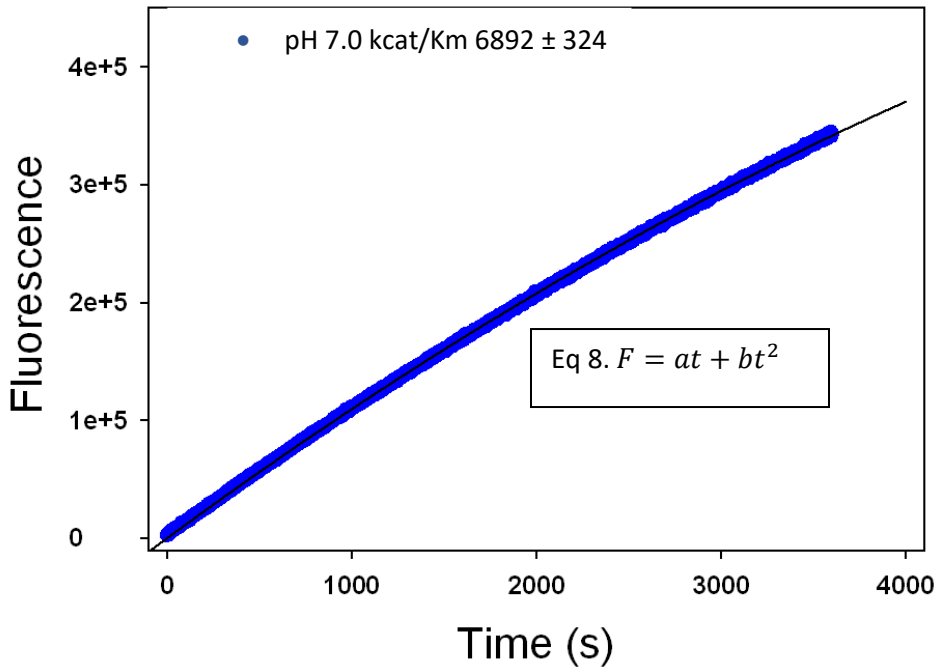

Figure 17. Reaction progress curve of ScOTU1 deubiquitinase with Ubiquitin-Rhodamine. Experimental data represented by the blue line and fit to Equation 8 is represented by the black line. A mixture of 50 nM ScOTU1, 250 nM Ubiquitin-Rhodamine, and 2 mM DTT in a reaction buffer consisting of 50 mM TRIS-HCl, 50 mM NaCl, at pH 7.0 were added to a 1 ml quartz cuvette. The mixture was incubated at 4°C for 1 hour and allowed to equilibrate to room temperature for 10 minutes before experiments began. Fluorescence measurements were done on the solution at an excitation wavelength of 485 nm and an emission wavelength of 535 nm.

Figure 18 shows the reaction progress curves for measurements at both pH 7.0 and pH 6.0. In this figure there is an observed decrease in the slope of the curve as the pH is decreased from pH 7.0 to 6.0. The specificity constants of and 1262 $M^{-1}s^{-1}$ for pH 6.0 is 42% lower than that measured at pH 7 (2180 $M^{-1}s^{-1}$) which is shown in Table 5.

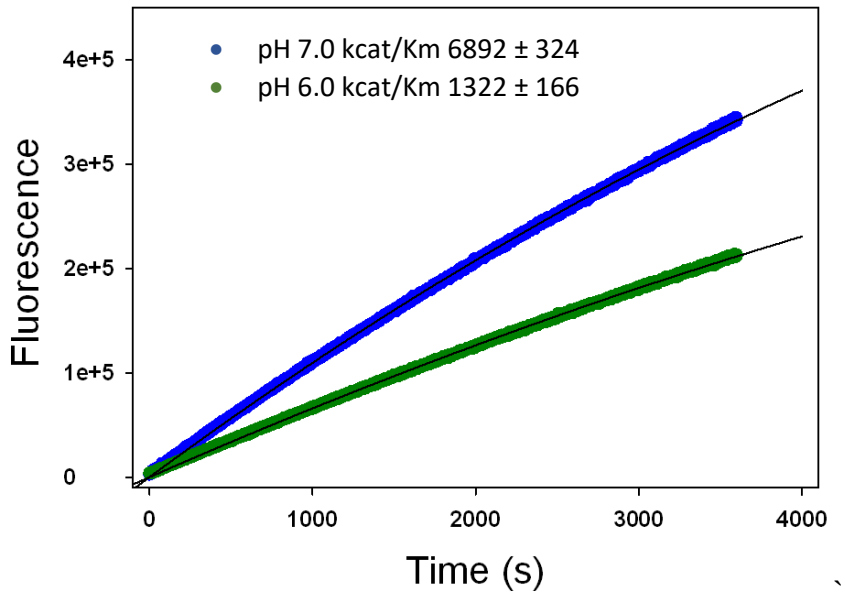

Figure 18. Reaction progress curve of ScOTU1 deubiquitinase with Ubiquitin-Rhodamine at pH 7.0 and 6.0. A mixture of 50 nM ScOTU1, 250 nM Ubiqutin-Rhodamine, and 2 mM DTT in ContBuffer[3] at pH 6.0 and 7.0 were added to a 1 ml quartz cuvette. Mixtures were incubated at 4°C for 1 hour and allowed to equilibrate to room temperature for 10 minutes before experiments began. Fluorescence measurements were done on the solutions at an excitation wavelength of 485 nm and an emission wavelength of 535 nm. The highlighted blue and green lines represent the experimental data for pH 7 and 6, respectively and the black lines represent the fit of the curves using equation 8.

Table 5. k_{cat}/K_M values calculated at pH 6.0 and 7.0. These values were determined using equations outlined in the Methods section and the fitting of the raw data was done using equation 8.

pH	k_{cat}/K_M ($M^{-1}s^{-1}$)
6.0	1322 ± 166
7.0	6892 ± 324

Figure 19, is a graphical representation of the k_{cat}/K_M measured between pH 6 and pH 7. The calculated specificity constants are tabulated in Table 6. The specificity constants remain similar from pH 7.75 to pH 6.5 with a decrease only happening at pH 6.25. The data were plotted using a logarithmic scale to reduce the difference between k_{cat}/K_M values that were calculated.

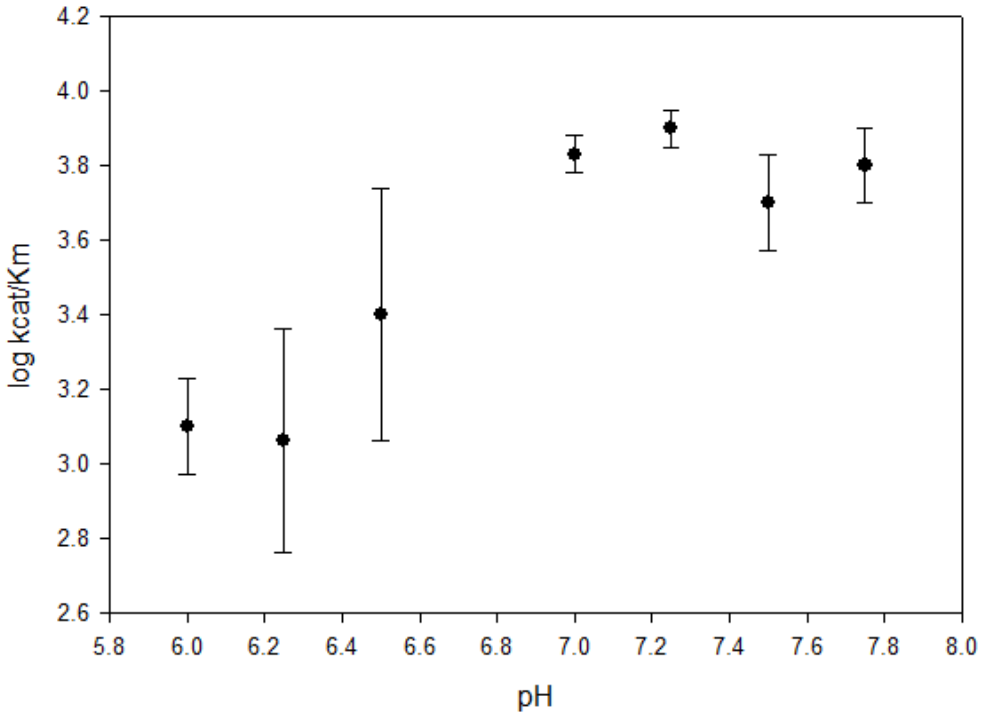

Figure 19. Log of k_{cat}/K_M as pH is increased for the enzymatic activity of ScOTU1 on Ubiquitin-Rhodamine.

Table 6. The log of k_{cat}/K_M values calculated from pH 6.0 to pH 7.75.These values were determined using equations outlined in Methods section and the fitting of the raw data was done using equation 8.

pH	Log [k_{cat}/K_M ($M^{-1}s^{-1}$)]
6.0	3.10 ± 0.13
6.25	3.06 ± 0.30
6.5	3.40± 0.34
7.0	3.83 ± 0.05
7.25	3.90 ± 0.05
7.5	3.70 ± 0.13
7.75	3.8 ± 0.10

3.3 Bis-ANS Hydrophobic Assay

Bis-Ans experiments were done at room temperature in solutions with pH values ranging from 7 to 9. A constant concentration of ScOTU1 and DTT was added to solutions of increasing Bis-ANS concentration to determine if alterations in pH would change the surface properties of ScOTU1 by measuring the variations in fluorescence of Bis-ANS monitored at 492 nm.

Figure 20 demonstrates the change in fluorescence intensity of free Bis-ANS at pH 7.5 as the dye concentration increases indicated by the black circles, in contrast to Bis-ANS bound to ScOTU1

at pH 7.5, indicated by the white circles. There is a slight increase in fluorescence of free Bis-ANS as the concentration is increased while the fluorescence increase is much greater when Bis-ANS is in a solution containing ScOTU1. Figure 20 also suggests that there is background fluorescence that needs to be corrected for when performing calculations on the raw fluorescence counts but the background is small enough that it does not greatly change the methodology outlined in the Materials and Methods section 2.3.

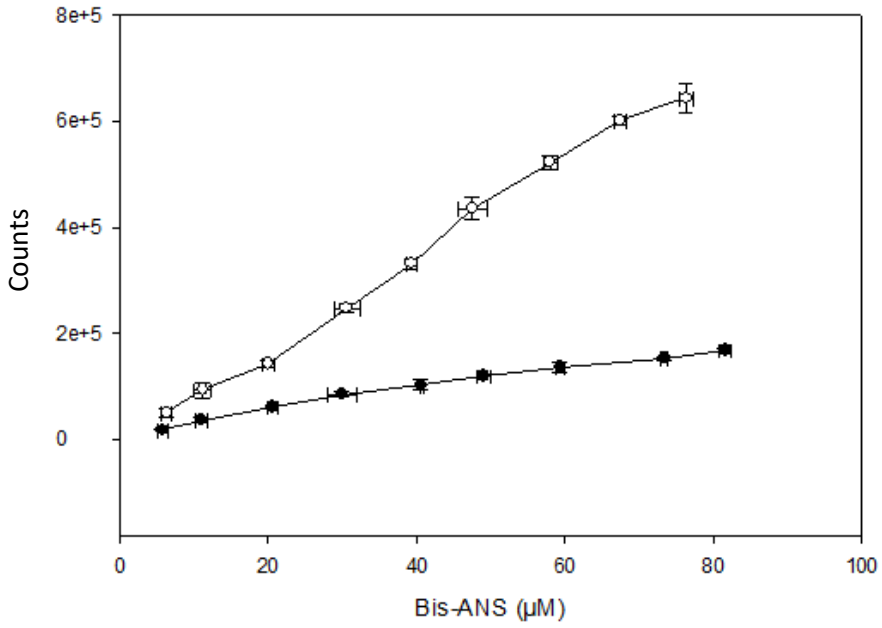

Figure 20. Fluorescence intensity vs concentration curve of free Bis-ANS (black) at increasing concentrations in a buffer consisting of 50 mM sodium phosphate dibasic and 50 mM sodium chloride (Bis-buffer^2) at pH 7.5. Bound Bis-ANS (white) consisted of a solution containing 0.5 μM ScOTU1 and 2 mM DTT in pH 7.5 Bis-buffer^2. Each solution was mixed and allowed to incubate at 4°C for 1 hour to allow for complete binding and thereafter allowed to incubate at room temperature for 10 minutes. An excitation wavelength of 350 nm was used with an emission wavelength of 492 nm using a 0.4 mm pathlength for the cuvette.

From pH 7 to 9, fluorescence *vs* Bis-ANS concentration curves were recorded with increasing increments of 0.25 pH units. The fluorescence intensity curves were fit by the four-parameter Hill regression model equation 2 in Section 2.3 of the Materials and Methods. The fitting of the experimental data by the models is exemplified in Figure 21 by the curves for the experiments at pH 9, 7.75, and 7 indicated by the dotted line, solid line, and dashed line respectively.

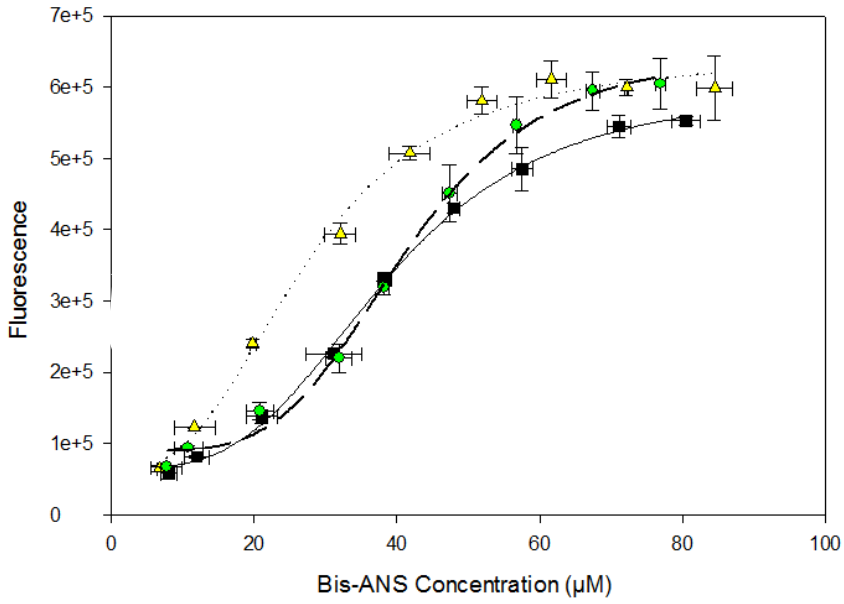

Figure 21. Regression model for the fit of the fluorescence intensity vs concentration curves of Bis-ANS at pH 9, 7.75, and 7.0 indicated by the yellow triangles and dotted line, black squares and solid line, and green circles and dashed line respectively.

The resultant parameters from the regression model were used to calculate the percentage of Bis-ANS bound to ScOTU1 at different pH values. Figure 21 displays the percentage of Bis-ANS bound to ScOTU1 as a function of increasing Bis-ANS concentration at pH values of 7, 7.5, and 9 indicated by the green circles, black squares, and yellow triangles respectively. A three-parameter Hill regression model was then used to fit the percentage-bound curves and to

calculate the dissociation constant at each pH as outlined in Materials and Methods section using equation 1. The fits of the percentage-bound curves are shown in Figure 22 as the dotted line, solid line, and dashed line for pH 9, 7.75, and 7.5 respectively. The dissociation constants K_d were then calculated from the parameters from the regression model and plotted as shown in Figure 23. There is some fluctuation of K_d between pH 7 to 8 with a significant outlier at pH 7.5 but above pH 8 the dissociation constants decrease significantly without much variation as shown in Table 7.

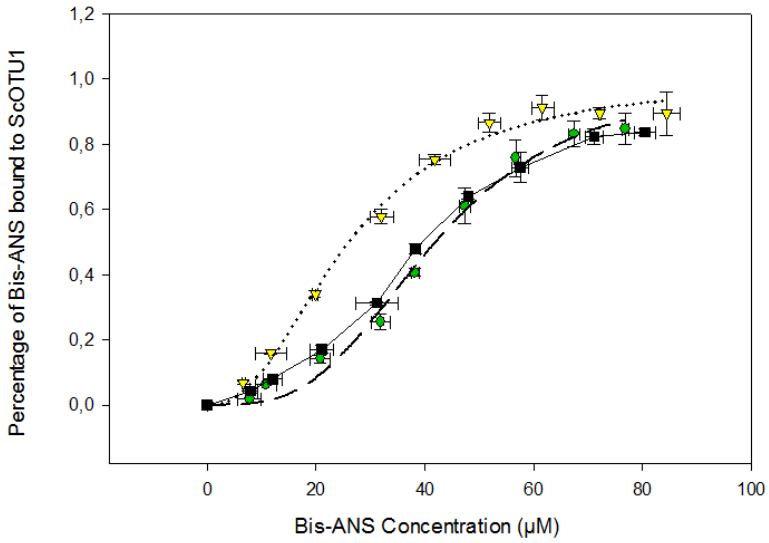

Figure 22. Percentage of Bis-ANS bound to ScOTU1 vs Bis-ANS concentration at pH 7.0, 7.75, and 9 indicated by the green circles, black squares, and yellow triangles respectively. Percentage bound values were corrected for the fluorescence of free Bis-ANS in solution.

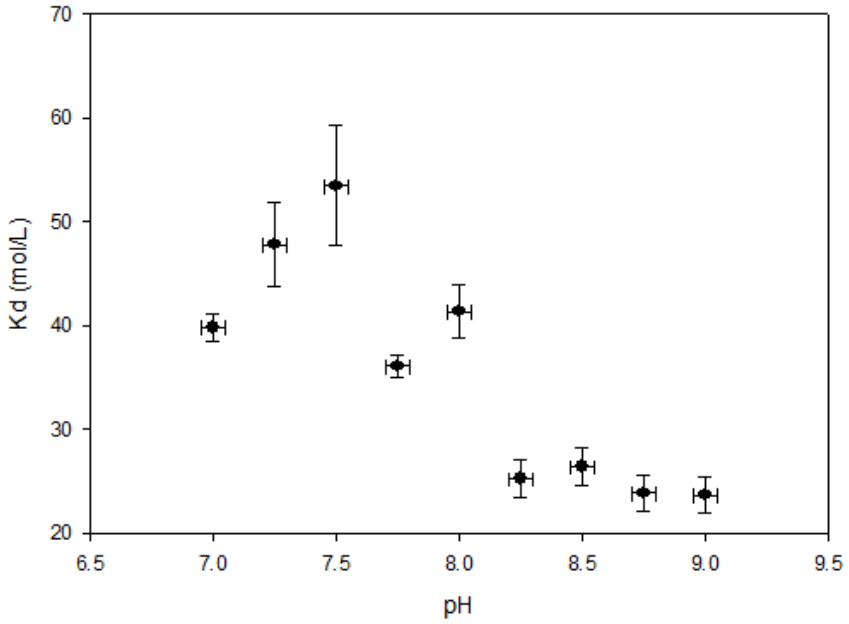

Figure 23. Dissociation constant of Bis-ANS binding to ScOTU1 at different pH values.

Chapter 4

Discussion

4.1 Overview

The ScOTU1 catalytic domain has been shown to exist in an opened active conformation and a closed inactive conformation that is thought to be partially dependent on two dynamic loop regions the first of which is a WGGA loop and a second is a FFY loop both of which arise from separate secondary structure regions of the protein. Both loops surround the catalytic cleft of the enzyme and form stabilizing bonds with ubiquitin[19]. This modulation of activity through loop-dependent dynamics is seen in otubain 2 a human deubiquitinating enzyme that is also dependent on a structurally similar OTU domain. Otubain 2 has a disordered loop region that is in an area where it can effectively sterically block binding of the OTU domain to ubiquitin[74]. The aforementioned loop regions in ScOTU1 are located in the same area as the loops in otubain 2 but in contrast to

the inhibitory effects of the otubain 2 loops the ScOTU1 loops have been shown to form stabilizing linkages with ubiquitin that reorient the terminal residues of ubiquitin to form associative interactions[19]. Taken together these two deubiquitinating enzymes show that the WGGA and FFY loop regions are most likely part of a conformational transition that enables the deubiquitinases to change conformation from an inactive to an active state or *vice versa* based on dynamic changes in the protein.

Two models have been proposed to explain the transition from an active to inactive state in ScOTU1[39]. The first model proposed the occurrence of conformational changes within free ScOTU1 before the interaction of the enzyme with a polyubiquitin molecule. This monomolecular model suggests that the catalytic cysteine residue is generally not accessible when ScOTU1 is free in solution. Only through rapid conformational changes can ScOTU1 temporarily open and expose the catalytic cleft and catalytic triad to solvent where polyubiquitin could then bind and result in the cleavage of the iso-peptide bonds in a polyubiquitin chain.

The second model[39] suggests an induced conformational change which would occur after an initial interaction or binding event between ScOTU1 and a polyubiquitin chain. This binding event would involve the stabilization of the ubiquitin-ScOTU1 interface by hydrophobic interactions, hydrogen bonding, and electrostatic interactions which would induce conformational changes within the protein. These interactions would open the catalytic cleft and provide access to the catalytic cysteine residue where cleavage could then occur.

In both models, a pH dependence was observed that showed that as pH was increased from pH 7 to 9 the binding of a small molecule probe aldrithiol-4 (DTDP), to the catalytic cysteine through the formation of a disulfide bond became more favourable. This suggested that at low pH there was reduced accessibility to the catalytic cysteine which meant that there might be important

protonation events at low pH that induced conformation changes in the enzyme causing it to adopt a closed conformational whereas at high pH the protein became more open and accessibility to the catalytic cysteine actually increased.

4.2 Bis-ANS

Bis-ANS is a hydrophobic surface probe that has been shown to increase its fluorescence quantum yield when bound to hydrophobic regions on proteins[48]. This method has been used extensively to study conformational dynamics of proteins under various conditions including pH titration experiments[60,75,76]. The dynamics of ScOTU1 have not up to this point been studied using a hydrophobic surface probe and the majority of the structural studies have been done using x-ray diffraction[48]. Prior to the initiation of hydrophobic probe studies with Bis-ANS the association between protein and Bis-ANS must be assessed to ensure that the affinity between the probe and protein is strong enough to produce a significant increase in fluorescence so that baseline fluorescence emission does not produce confounding results[75]. The fluorescence of free Bis-ANS was studied and compared to Bis-ANS in solution with ScOTU1 as shown in Figure 20. The change in quantum yield confirmed that the fluorescence as a result of binding increased the quantum yield by a factor of four when comparing the free Bis-ANS fluorescence to the bound fluorescence. In other studies, the increase in fluorescence yield ranged from a factor of four to eight which indicates that the measured fluorescence increase was enough to proceed with the hydrophobic probe studies[75,76].

The hydrophobic probe experiments were then extended to study the binding of increasing concentrations Bis-ANS to ScOTU1 at different pH values. These Bis-ANS titration experiments are commonly used to retrieve biophysical parameters such as association and dissociation constants, K_a and K_d respectively, and quantitative measures like the dimensionless Hill coefficient

n that provide insight into the dynamics and nature of the protein as binding occurs[60,75,76]. As Figure 21 indicates, the binding of increasing concentrations of Bis-ANS to ScOTU1 follows a sigmoidal dependence on Bis-ANS concentration. Sigmoidal binding curves are typically characteristic of a positive cooperative binding process where the association of one ligand molecule to an enzyme causes structural changes that influence the association of the next ligand molecule by increasing the affinity of binding[63].

It is possible that sigmoidal binding curves do not in reality reflect positive cooperative binding, so to ensure that cooperativity is occurring during binding the Hill coefficient *n* must be calculated by fitting the sigmoidal curve to a Hill equation as described in the Materials and Methods section. A Hill coefficient that is less than one indicates negative cooperativity wherein a ligand binding to an enzyme decreases the affinity of the enzyme for ligands that try to bind afterwards. A Hill coefficient equal to one indicates that ligand binding is not cooperative which means that the affinity of an enzyme towards a ligand does not increase as binding occurs and a Hill coefficient greater than one indicates cooperative binding which means that once a ligand binds to an enzyme it increases the affinity of the enzyme towards other ligands[77]. While the Hill coefficient is thought to provide a measure of the amount of binding sites present on an enzyme and their degree of cooperativity it is important to note that it is best thought of as a interaction coefficient which only reflects the amount of cooperativity that occurs among different ligand binding sites without specifying how many binding site are present[77]. The binding of oxygen to haemoglobin for example is often mentioned when discussing positive cooperativity and that system has a Hill coefficient that is typically between 1.7-3.2 whereas there are 4 binding sites that have positive cooperativity[78]. Fitting the sigmoidal curves produced from the binding of Bis-ANS to ScOTU1

for pH values ranging from 7 to 9 resulted in Hill coefficients between 1.85-3.09 as shown in Table 7.

Table 7. Hill coefficients n for the fitting of the sigmoidal curves from pH 7 to 9 using Bis-ANS

pH	Hill Coefficient *n*
7.0	3.09 ± 0.79
7.25	2.16 ± 0.34
7.5	1.85 ± 0.21
7.75	3.06 ± 0.46
8.0	2.40 ± 0.41
8.25	1.96 ± 0.29
8.5	2.16 ± 0.37
8.75	2.15 ± 0.38
9.0	2.72 ± 0.51

Based on the data in Table 7 it is reasonable to classify the binding of Bis-ANS to ScOTU1 as one where cooperativity does occur between a number of hydrophobic binding sites.

The dissociation constant K_d is another important biophysical parameter that was calculated by fitting the sigmoidal binding data with the Hill equation. K_d can be used to estimate the strength of interaction between the solvent-accessible apolar regions on the surface of a protein and Bis-ANS[79]. A small K_d indicates a strong binding affinity between a ligand and an enzyme whereas a

large K_d indicates weak binding affinity between a ligand and an enzyme[60,75,76]. As shown in Figure 21 of the Results section the dissociation constants ranged from 23 µM-53 µM where the upper limit of 53 µM indicated a binding interaction that was almost a factor of two weaker than the lower limit of 23 µM.

The dissociation constant K_d in conjunction with the Hill coefficient *n* can provide a greater understanding of the dynamics that occur within ScOTU1 and these results can further support or disprove the feasibility of the models discussed previously. The Hill coefficients calculated for various pH values in the titration of ScOTU1 by Bis-ANS suggest that the binding of Bis-ANS to ScOTU1 occurs through a cooperative mechanism where binding is mediated by hydrophobic and electrostatic interactions. In their studies of the binding interface of ScOTU1 and Ubiquitin Messick et al. (2005) listed three key regions of interaction between ScOTU1 and Ubiquitin each exploiting hydrophobic and electrostatic interactions.

Region one of ScOTU1 consists of a small lobe where two scaffolding α-helices α2 and α4 interact with a ubiquitin-recognition helix α3. Ile^{57} of ScOTU1, also in region one binds to hydrophobic patch on ubiquitin and is part of an extensive hydrogen bonding network[19]. Region two of ScOTU1 forms an indirect hydrogen bonding network between Asn^{206} and Glu^{207} of ScOTU1 and a loop within 4 Å of the ubiquitin core[19]. Region three consists of the catalytic cleft and is where the most abundant interactions occur between ScOTU1 and ubiquitin. The interactions in region three are primarily mediated by two loops regions, the WGGA loop between α4 and α5 and a second loop consisting of Phe^{218}, Tyr^{223}, and Phe^{205}. Both loops aid in the insertion of the carboxyl terminus of ubiquitin into the catalytic cleft where the active site cysteine of ScOTU1 resides. All three of these regions taken together make many important contacts with ubiquitin that enable the binding and subsequent cleavage of the iso-peptide bonds of polyubiquitin molecules.

When mutational studies were completed on the key interaction residues of each region, interesting results were found[19]. In regions 1 and 3 where hydrophobic interactions are very important, the mutation of the residues involved in the hydrophobic binding interactions resulted in almost complete loss of wild type activity whereas in region 2, where the interaction was primarily of a hydrogen bonding nature the mutant showed 50% of wild type activity[19]. This again suggested that the hydrophobic interactions between ScOTU1 and ubiquitin are the most important catalytic activity-mediating interactions. These findings, in addition to the Hill coefficients above 1, suggest strongly that model one is not plausible as there needs to be binding interactions for the conformation of ScOTU1 to change so that ubiquitin can enter the catalytic cleft. These binding interactions are mediated by the formation of a ubiquitin-ScOTU1 interface which most likely forms cooperatively.

In experiments that measured the initial slopes of the disulfide bond formation between the catalytic cysteine residue and the small molecule probe DTDP[80] over the pH range from 7 to 9, a marked decrease was observed in the initial slopes as the pH was decreased to a physiological level[39]. At pH 8 and below there was a significant increase in the dissociation constants as shown in Table 6 from an average value of 25 μM at pH 8.25 and above and 40 μM at pH 8 and below. This increase at pH 8 and below could indicate that the protonation of certain residues induces structural changes within ScOTU1 that promote a closed conformation. Additionally, the catalytic cysteine residues are buried deep within the catalytic cleft at physiological pH[19]**.** The reduced accessibility of the small molecule probe is likely due to these conformation changes that occur at lower pH which make it less likely that the DTDP can obtain access to the tightly closed catalytic cleft. In contrast at higher pH values, ScOTU1 has been shown to adopt a much more open conformation where the hydrophobic regions are readily accessible as shown by the much lower

dissociation constants. This could provide the probe much easier access for binding to cysteine. Furthermore, at a pH above 8, which is close to the pKa of cysteine, the cysteine may be deprotonated without the aid of the catalytic triad again making binding to DTDP more likely.

It is most likely due to the interaction between regions 1, 2, and 3 that ubiquitin can enter the catalytic cleft to gain access to the catalytic triad. A small molecule probe such as DTDP cannot form those same hydrophobic interactions and so in the closed conformation at pH 7 is not able to gain access to the catalytic cysteine residue. Additionally, despite Bis-ANS being able to bind to hydrophobic patches on ScOTU1 it cannot induce the same conformational changes that occur when ScOTU1 binds with ubiquitin. The more closed conformation could arise at lower pH values, due to the separation of important amino acids sequences such as the FFY loop region where all three residues originate from entirely separate secondary structure elements. This increased separation could also displace the catalytic triad amino acids of aspartic acid and histidine residues away from the catalytic cysteine residue[19].

4.2 Ubiquitin Rhodamine

Ubiquitin Rhodamine is a more natural substrate for ScOTU1 than either the hydrophobic surface probe Bis-ANS or the small molecule probe DTDP and was applied in these experiments to determine if using a substrate that could potentially mimic the hydrophobic and electrostatic interactions that ScOTU1 forms in *vivo* with polyubiquitin chains would enable activity or accessibility to the catalytic cysteine at pH 8 and below.

As shown in Figure 17, at pH 7 the cleavage of ubiquitin rhodamine occurred successfully at the RLGG sequence within the linker region between the ubiquitin and rhodamine molecules which is the sequence that ScOTU1 recognizes and cleaves in natural polyubiquitin molecules[81]. Table 6 and Figure 19 show that k_{cat}/K_m does not change appreciably with pH. This seems to indicate that

in contrast to what was seen with both Bis-ANS and DTDP, there was now access to the catalytic site at lower pH values.

The new activity range means that perhaps Model 2 described earlier was appropriate. Ubiquitin may interact with a closed ScOTU1 molecule which forces it, through cooperative conformational changes, to adopt an active conformation by binding and interacting at hydrophobic patches. This is a plausible explanation because, as observed before, the protein was initially in a closed conformation where even a hydrophobic probe could not gain access to the catalytic cleft. Bis-ANS may bind to the same patches that ubiquitin does but it is not able to cause ScOTU1 to adopt an active open conformation. It is only through the binding and interaction of all the sites cooperatively that the active site cysteine becomes available as exemplified by the ubiquitin-rhodamine experiments.

Taken together, the conformational dynamics of ScOTU1 are pH dependent where at a low pH it adopts a closed conformation, possibly due to the separation of important protein sequences that allow the enzyme to adopt the active conformation or due to protonation of certain residues that close the protein. The high dissociation constant may simply mean that unless a ubiquitin chain has the correct linkages and orientation then ScOTU1 cannot cleave it as it will not bind strongly which makes sense biologically. This could be a method to ensure strong specificity for target proteins at physiological pH. Future studies will have to be completed to determine if in fact Bis-ANS will competitively inhibit the binding and cleavage of ubiquitin-rhodamine by ScOTU1 by binding to the same hydrophobic patches that ubiquitin typically does. These experiments could provide insight into how the multiple regions on ubiquitin interact with ScOTU1 and induce the opening of its structure.

Chapter 5

Summary and Future Directions

In the work presented in this thesis the catalytic domain of OUT1 was investigated. ScOTU1 was successfully over-expressed and purified by excluding an overnight dialysis step and instead directly injecting the protein solution onto a size-exclusion column for rapid buffer exchange. Specificity constant k_{cat}/K_m was calculated based on pH-dependent Ubiqutin-Rhodamine 110 continuous assays where we did not see a pH dependent change in catalysis as the solution pH was increased from 6.25 to 7.75. The range of log k_{cat}/K_m values varied by at most 0.3 $M^{-1}s^{-1}$ which means the protein remains open at a much lower pH. These results did not agree with the strong pH-dependent decrease in turnover rate k_{cat} seen using a small molecule probe DTDP as shown in Figure 5a where, at pH 7, there was effectively no accessibility to the catalytic cysteine residues due to the protein adopting a closed conformation.

Bis-ANS experiments were used to calculate the Hill coefficient which showed that the binding of Bis-ANS occurred through a cooperative mechanism. The dissociation constant K_d was calculated based on Bis-ANS experiments which showed that at pH between 8.25 to 9 the K_d values averaged 25 mol/L whereas at pH 7 to 8.25 the values averaged 40 mol/L. This showed that there was a clear transition to a closed conformation with less hydrophobic patches available for binding as the pH was decreased.

The results from both the Ubiquitin-Rhodamine 110 and Bis-ANS experiments taken together suggest that free in solution at physiological pH ScOTU1 adopts a closed conformation that it will only open at physiological pH when it forms favourable electrostatic and hydrophobic interactions with ubiquitin.

The future directions for studying OTU1 could utilize competitive enzyme assays between Ubiquitin and Bis-ANS which would enable us to determine if Bis-ANS is actively binding to some of the same hydrophobic patches that Ubiquitin utilizes to form interactions with ScOTU1. Nuclear Magnetic Resonance experiments could be utilized by applying Principal Component Analysis to monitor structural changes of the protein as the pH is varied using heteronuclear sequential quantum correlation (HSQC) which could allow us to observe more specifically where transitions occur from a closed to open conformation and which residues are playing a large part in those transitions. Bis-ANS and Ubiquitin-Rhodamine 110 experiments might then be repeated similarly to the experiments outlined in this thesis but either the ubiquitin like domain or zinc binding domain can remain attached to ScOTU1 to see how multiple domains modulate or change the activity of the enzyme.

Citations

1.Frauenfelder, H. *et al.* A unified model of protein dynamics. *Proc. Natl. Acad. Sci.* **106**, 5129–5134 (2009).

2.Austin, R. H., Beeson, K. W., Eisenstein, L., Frauenfelder, H. & Gunsalus, I. C. Dynamics of Ligand Binding to Myoglobin. *Biochemistry* **14**, 5355–5373 (1975).

3.Lin, M. M. & Zewail, A. H. Hydrophobic forces and the length limit of foldable protein domains. *Proc. Natl. Acad. Sci.* **109**, 9851–9856 (2012).

4.Zwanzig, R., Szabo, A. & Bagchi, B. Levinthal's paradox. *Proc. Natl. Acad. Sci. U. S. A.* **89**, 20–22 (1992).

5.Srivastava, A., Nagai, T., Srivastava, A., Miyashita, O. & Tama, F. Role of computational methods in going beyond x-ray crystallography to explore protein structure and dynamics. *Int. J. Mol. Sci.* **19**, (2018).

6.Marion, D. An introduction to biological NMR spectroscopy. *Mol. Cell. Proteomics* **12**, 3006–3025 (2013).

7.Rigden, D. J. *From Protein Structure to Function with Bioinformatics*. *From Protein Structure to Function with Bioinformatics: Second Edition* (Springer Netherlands, 2017). doi:10.1007/978-94-024-1069-3

8.Camilloni, C. *et al.* Towards a structural biology of the hydrophobic effect in protein folding. *Sci. Rep.* **6**, 1–9 (2016).

9.Guo, S. *et al.* Structure of a 1.5-MDa adhesin that binds its Antarctic bacterium to diatoms and ice. *Sci. Adv.* **3**, e1701440 (2017).

10.Basu, M. K., Poliakov, E. & Rogozin, I. B. Domain mobility in proteins: functional and evolutionary implications. *Brief. Bioinform.* **10**, 205–216 (2008).

11.P. Bagowski, C., Bruins, W. & J.W. te Velthuis, A. The Nature of Protein Domain Evolution: Shaping the Interaction Network. *Curr. Genomics* **11**, 368–376 (2010).

12.Yanez Orozco, I. S. *et al.* Identifying weak interdomain interactions that stabilize the supertertiary structure of the N-terminal tandem PDZ domains of PSD-95. *Nat. Commun.* **9**, 1–11 (2018).

13.Santacruz-Perez, C. *et al.* A specific interdomain interaction preserves the structural and binding properties of the ModA protein from the phytopathogen Xanthomonas citri domain interaction and transport in ModA. *Arch. Biochem. Biophys.* **539**, 20–30 (2013).

14 Csermely, P., Palotai, R. & Nussinov, R. Induced fit, conformational selection and independent dynamic segments: an extended view of binding events. *Trends Biochem. Sci.* **35**, 539–546 (2010).

15Trizac, E., Levy, Y. & Wolynes, P. G. Capillarity theory for the fly-casting mechanism. *Proc. Natl. Acad. Sci. U. S. A.* **107**, 2746–2750 (2010).

16Johnson, K. A. Role of induced fit in enzyme specificity: A molecular forward/reverse switch. *J. Biol. Chem.* **283**, 26297–26301 (2008).

17 Shoemaker, B. A., Portman, J. J. & Wolynes, P. G. Speeding molecular recognition by using the folding funnel: The fly-casting mechanism. *Proc. Natl. Acad. Sci. U. S. A.* **97**, 8868–8873 (2000).

18Paul, F. & Weikl, T. R. How to Distinguish Conformational Selection and Induced Fit Based on Chemical Relaxation Rates. *PLoS Comput. Biol.* **12**, 1–17 (2016).

19.Messick, T. E. *et al.* Structural basis for ubiquitin recognition by the Otu1 ovarian tumor domain protein. *J. Biol. Chem.* **283**, 11038–11049 (2008).

20.Kim, S. J. *et al.* Structural Basis for Ovarian Tumor Domain-containing Protein 1 (OTU1) Binding to p97/Valosin-containing Protein (VCP). *J. Biol. Chem.* **289**, 12264–12274 (2014).

21.Toma, A. *et al.* Structural Basis for Ubiquitin Recognition by Ubiquitin-Binding Zinc Finger of FAAP20. *PLoS One* **10**, e0120887 (2015).

22.Vernet, T. *et al.* Structural and Functional Roles of Asparagine 175 in the Cysteine Protease Papain. *J. Biol. Chem.* **270**, 16645–16652 (1995).

23. Swain, C., 2020. *Cysteine Protease Inhibitors, Cambridge Medchem Consulting*. [online] Cambridge MedChem Consulting. Available at: https://www.cambridgemedchemconsulting.com/resources/hit_identification/focus/cysteine_protease_inhibitors.html [Accessed 13 July 2020].

24.Grau-Bové, X., Sebé-Pedrós, A. & Ruiz-Trillo, I. The eukaryotic ancestor had a complex ubiquitin signaling system of archaeal origin. *Mol. Biol. Evol.* **32**, 726–739 (2015).

25.Hochstrasser, M. Evolution and function of ubiquitin-like protein-conjugation systems. *Nat. Cell Biol.* **2**, E153–E157 (2000).

26.Pickart, C. M. Mechanisms underlying ubiquitination. *Annu. Rev. Biochem.* **70**, 503–33 (2001).

27.Sadowski, M., Suryadinata, R., Tan, A. R., Roesley, S. N. A. & Sarcevic, B. Protein monoubiquitination and polyubiquitination generate structural diversity to control distinct biological processes. *IUBMB Life* **64**, 136–142 (2012).

28.Mevissen, T. E. T. *et al.* OTU Deubiquitinases Reveal Mechanisms of Linkage Specificity and Enable Ubiquitin Chain Restriction Analysis. *Cell* **154**, 169–184 (2013).

29.Wickliffe, K. E., Williamson, A., Meyer, H. J., Kelly, A. & Rape, M. K11-linked ubiquitin chains as novel regulators of cell division. *Trends Cell Biol.* **21**, 656–663 (2011).

30.Ebner, P., Versteeg, G. A. & Ikeda, F. Ubiquitin enzymes in the regulation of immune responses. *Crit. Rev. Biochem. Mol. Biol.* **52**, 425–460 (2017).

31.Schneider, W. M., Chevillotte, M. D. & Rice, C. M. Interferon-Stimulated Genes: A Complex Web of Host Defenses. *Annu. Rev. Immunol.* **32**, 513–545 (2014).

32.Ruggiano, A., Foresti, O. & Carvalho, P. ER-associated degradation: Protein quality control and beyond. *J. Cell Biol.* **204**, 869–879 (2014).

33.Bodnar, N. & Rapoport, T. Toward an understanding of the Cdc48/p97 ATPase. *F1000Research* **6**, 1318 (2017).

34.Furtado, A. R. *et al.* The chlamydial OTU domain-containing protein ChlaOTU is an early type III secretion effector targeting ubiquitin and NDP52. *Cell. Microbiol.* **15**, 2064–2079 (2013).

35.Bailey-Elkin, B. A., van Kasteren, P. B., Snijder, E. J., Kikkert, M. & Mark, B. L. Viral OTU Deubiquitinases: A Structural and Functional Comparison. *PLoS Pathog.* **10**, 1–6 (2014).

36.Wright, H. R., Turner, A. & Taylor, H. R. Trachoma. *Lancet* **371**, 1945–1954 (2008).

37.Blasi, F., Tarsia, P. & Aliberti, S. Chlamydophila pneumoniae. *Clin. Microbiol. Infect.* **15**, 29–35 (2009).

38.Grassetti, D. R. & Murray, J. F. Determination of sulfhydryl groups with 2,2′- or 4,4′-dithiodipyridine. *Arch. Biochem. Biophys.* **119**, 41–49 (1967).

39.Hutchings, R. *Probing the active site of the S. Cerevisiae OTU1 Deubiquitinase*. *Unpublished* (2017).

40.Lakowicz, J. R. *Principles of Fluorescence Spectroscopy*. *Analytical and Bioanalytical Chemistry* **390**, (Springer US, 2006).

41. Abramowitz, M. & Davidson, M., 2020. *Fluorescence Filters*. [online] Olympus-Lifescience. Available at :<https://www.olympus-lifescience.com/en/microscope-resource/primer/techniques/fluorescence/filters/> [Accessed 13 July 2020].

42.Lodge, J. P. Fluorescence Spectrophotometry. in *Methods of Air Sampling and Analysis* 187–190 (Lewis Publishers, 2017). doi:10.1201/9780203747407-29

43.Delsart, C. & Pelletier-Allard, N. Probabilities for radiative and nonradiative decay of Pr 3+ ion in LaAlO 3. *J. Phys. C Solid State Phys.* **6**, 1277–1291 (1973).

44.D. A. Skoog, et al. *Principles of Instrumental Analysis 6th Edition*, (Thomson Brooks/Cole. 2007).

45.Hall, P. J. The Pauli Exclusion Principle and the Foundations of Chemistry. *Synthese* **69**, 267–272 (1986).

46. D. C. Harris and M.D. Bertolucci. *Symmetry and Spectroscopy, An Introduction to Vibrational and Electronic Spectroscopy (*Dover Publications, Inc., New York. 1989).

47. 1. Li, R. & Li, C. Photocatalytic Water Splitting on Semiconductor-Based Photocatalysts. in *Advances in Catalysis* 1–57 (Elsevier, 2017). doi:10.1016/bs.acat.2017.09.001

48.Hawe, A., Sutter, M. & Jiskoot, W. Extrinsic fluorescent dyes as tools for protein characterization. *Pharm. Res.* **25**, 1487–1499 (2008).

49.Fu, Y. & Finney, N. S. Small-molecule fluorescent probes and their design. *R. Soc. Chem.* **8**, 29051–29061 (2018).

50.Zheng, H. *et al.* Characterization of the deubiquitination activity and substrate specificity of the chicken ubiquitin-specific protease 1/USP associated factor 1 complex. *PLoS One* **12**, 1–22 (2017).

51.Hassiepen, U. *et al.* A sensitive fluorescence intensity assay for deubiquitinating proteases using ubiquitin-rhodamine110-glycine as substrate. *Anal. Biochem.* **371**, 201–207 (2007).

52. Ubiquitin & Derivatives. *Biosyntan* (2020). at <https://www.biosyntan.de/ubiquitin-derivatives/ubiquitin-derivatives/>

53.Gold, V. Glossary of terms used in physical organic chemistry. *Pure Appl. Chem.* **51**, 1725–1801 (1979).

54. Sigma Aldrich. 2020. *4,4'-Dianilino-1,1'-Binaphthyl-5,5'-Disulfonic Acid Dipotassium Salt*. [online] Available at: https://www.sigmaaldrich.com/catalog/product/sigma/d4162?lang=en&region=CA&gclid=Cj0KCQjw_absBRD1ARIsAO4_D3vsCw1TBMmlZTGLduF32zRa4Vxh2Lj9srCvW58hLH3rn4p-6J7Jbo0aAooqEALw_wcB [Accessed 13 July 2020].

55.Das, K., Sarkar, N., Nath, D. & Bhattacharyya, K. Non-radiative pathways of anilino-naphthalene sulphonates: Twisted intramolecular charge transfer versus intersystem crossing. *Spectrochim. Acta Part A Mol. Spectrosc.* **48**, 1701–1705 (1992).

56.Slavík, J. Anilinonaphthalene sulfonate as a probe of membrane composition and function. *BBA - Rev. Biomembr.* **694**, 1–25 (1982).

57.Dielectric Constants of Liquids. *[online] Available at*: https://www.engineeringtoolbox.com/liquid-dielectric-constants-d_1263.html [Accessed 13 July 2020]

58.Dimethyl Sulfoxide (DMSO). *Sigma Aldrich [online] Available at*: https://www.sigmaaldrich.com/chemistry/solvents/dimethyl-sulfoxide-center.html [Accessed 13 July 2020]

59.Dynamic Viscosity of common Liquids. *[online] Available at*: https://www.engineeringtoolbox.com/absolute-viscosity-liquids-d_1259.html [Accessed 13 July 2020]

60.Sheluho, D. & Ackerman, S. H. An Accessible Hydrophobic Surface Is a Key Element of the Molecular Chaperone Action of Atp11p. *J. Biol. Chem.* **276**, 39945–39949 (2001).

61.Ventura, G. *et al*. pH-dependent conformational changes in the HCV NS3 protein modulate its ATPase and helicase activities. *PLoS One* **9**, e115941 (2014).

62.Ron, E. Z., Kohler, R. E. & Davis, B. D. Polysomes Extracted from Escherichia coli by Freeze-Thaw-Lysozyme Lysis. *Science (80-.).* **153**, 1119–1120 (1966).

63.Gómez-Cambronero, J. The Oxygen Dissociation Curve of Hemoglobin: Bridging the Gap between Biochemistry and Physiology. *J. Chem. Educ.* **78**, 757 (2001).

64.Stefan, M. I. & Le Novère, N. Cooperative Binding. *PLoS Comput. Biol.* **9**, e1003106 (2013).

65.Gadagkar, S. R. & Call, G. B. Computational tools for fitting the Hill equation to dose-response curves. *J. Pharmacol. Toxicol. Methods* **71**, 68–76 (2015).

66.Taylor Series. *Mathsisfun.com* (2020). at https://www.mathsisfun.com/algebra/taylor-series.html

67.García-Fruitós, E. *Insoluble Proteins*. *Insoluble Proteins: Methods and Protocols* **1258**, (Springer New York, 2015).

68.Hedberg, Y. S. *et al.* Synergistic effects of metal-induced aggregation of human serum albumin. *Colloids Surfaces B Biointerfaces* **173**, 751–758 (2019).

69.Oza, R., Shah, N. & Patel, S. Extraction of nickel from spent catalyst using EDTA as chelating agent. *Nat. Environ. Pollut. Technol.* **10**, 197–200 (2011).

70. G- Role of the Isoelectric Point of a Protein in its Purification. *G-Biosciences* (2020). at https://info.gbiosciences.com/blog/bid/149959/what-is-the-role-of-the-isoelectric-point-of-a-protein-in-its-purification

71.Studier, F. W. Protein production by auto-induction in high-density shaking cultures. *Protein Expr. Purif.* **41**, 207–234 (2005).

72. Studier, F. W. Recipes and stock solutions described in Protein Expression and Purification. *Protein Expr. Purif.* **41**, 207–234 (2005).

73.Inada, T., Kimata, K. & Aiba, H. Mechanism responsible for glucose-lactose diauxie in Escherichia coli: Challenge to the cAMP model. *Genes to Cells* **1**, 293–301 (1996).

74.Nanao, M. H. *et al.* Crystal structure of human otubain 2. *EMBO Rep.* **5**, 783–788 (2004).

75.Chatterjee, T. *et al.* Accessory cholera enterotoxin, ace, from vibrio cholerae: Structure, Unfolding, and Virstatin Binding. *Biochemistry* **50**, 2962–2972 (2011).

76.Möller, M. & Denicola, A. Study of protein-ligand binding by fluorescence. *Biochem. Mol. Biol. Educ.* **30**, 309–312 (2002).

77.Weiss, J. N. The Hill equation revisited: uses and misuses. *FASEB J.* **11**, 835–841 (1997).

78.Barcroft, J. The Combinations of Haemoglobin with Oxygen and with Carbon Monoxide. II. *Biochem. J.* **7**, 481–491 (1913).

79.Horowitz, P., Prasad, V. & Luduena, R. F. Bis(1,8-anilinonaphthalenesulfonate). A novel and potent inhibitor of microtubule assembly. *J. Biol. Chem.* **259**, 14647–14650 (1984).

80.Hermanson, G. T. The Reactions of Bioconjugation. in *Bioconjugate Techniques* 229–258 (Elsevier, 2013). doi:10.1016/B978-0-12-382239-0.00003-0

81.Hassiepen, U. *et al.* A sensitive fluorescence intensity assay for deubiquitinating proteases using ubiquitin-rhodamine110-glycine as substrate. *Anal. Biochem.* **371**, 201–20